Asian Journal of Pharmaceutical Sciences 18 (2023) 100873

Available online at www.sciencedirect.com

ScienceDirect

journal homepage: www.elsevier.com/locate/AJPS

Review Article

# Smart stimuli-responsive drug delivery systems in spotlight of COVID-19

*Zeinab Najjari, Farzaneh Sadri, Jaleh Varshosaz**

*Novel Drug Delivery Systems Research Center, Department of Pharmaceutics, School of Pharmacy and Pharmaceutical Sciences, Isfahan University of Medical Sciences, Isfahan, Iran*

ARTICLE INFO

*Article history:*
Received 18 May 2023
Revised 15 August 2023
Accepted 11 October 2023
Available online 1 December 2023

*Keywords:*
Stimuli-responsive
Smart drug delivery system
Biomedical applications
Endogenous and exogenous stimuli
COVID-19

ABSTRACT

The world has been dealing with a novel severe acute respiratory syndrome (SARS-CoV-2) since the end of 2019, which threatens the lives of many people worldwide. COVID-19 causes respiratory infection with different symptoms, from sneezing and coughing to pneumonia and sometimes gastric symptoms. Researchers worldwide are actively developing novel drug delivery systems (DDSs), such as stimuli-responsive DDSs. The ability of these carriers to respond to external/internal and even multiple stimuli is essential in creating "smart" DDS that can effectively control dosage, sustained release, individual variations, and targeted delivery. To conduct a comprehensive literature survey for this article, the terms "Stimuli-responsive", "COVID-19″ and "Drug delivery" were searched on databases/search engines like "Google Scholar", "NCBI", "PubMed", and "Science Direct". Many different types of DDSs have been proposed, including those responsive to various exogenous (light, heat, ultrasound and magnetic field) or endogenous (microenvironmental changes in pH, ROS and enzymes) stimuli. Despite significant progress in DDS research, several challenging issues must be addressed to fill the gaps in the literature. Therefore, this study reviews the drug release mechanisms and applications of endogenous/exogenous stimuli-responsive DDSs while also exploring their potential with respect to COVID-19.



## 1. Introduction

Coronaviruses belong to the Coronaviridae family, Coronavirinae subfamily. Coronaviruses (65–125 nm in diameter) are enveloped RNA viruses that contain a single positive-stranded RNA genome approximately 26–32 kilobases in length and are commonly known to cause respiratory tract or intestinal infections in mammals (*e.g.*, humans) and animals [1]. The Coronavirinae subfamily is classified into four groups by phylogenetic clustering: alpha ($\alpha$), beta ($\beta$), gamma ($\gamma$) and delta ($\delta$) coronavirus [1]. Specific genes in downstream regions of ORF1 in all coronaviruses encode variant proteins for virus formation and replication [2]. The crown-like spike (S) glycoprotein on the virus's outer surface, which causes the virus to be named coronavirus,

* Corresponding author.
*E-mail address:* varshosaz@pharm.mui.ac.ir (J. Varshosaz).
Peer review under responsibility of Shenyang Pharmaceutical University.

https://doi.org/10.1016/j.ajps.2023.100873

mediates attachment to the host cell receptor on the cell membrane and entry to host cells. HCoV-NL63 and SARS-coronavirus recognize angiotensin-converting enzyme 2 (ACE2) as a critical receptor for entry to host cells, while MERS-coronavirus recognize dipeptidyl peptidase 4 (DPP4) [3].

So far, seven coronaviruses could infect humans, including common human coronaviruses (the cause of self-resolving infection) and others (the cause of lethal respiratory infections). Common human coronaviruses are HCoV-229E ($\alpha$-coronavirus), HCoV-NL63 ($\alpha$-coronavirus), HCoV-OC43 ($\beta$-coronavirus) and HCoV-HKU1 ($\beta$-coronavirus) strains that the HCoV-229E virus was identified as the first human coronavirus in the mid-1960s [4]. Also other coronaviruses are $\beta$-coronaviruses including severe acute respiratory syndrome coronavirus (SARS-CoV), Middle East Respiratory Syndrome coronavirus (MERS-CoV), and currently identified SARS-CoV-2 [5]. In December 2019, the new coronavirus was named SARS-CoV-2 or COVID-19 by WHO on Feb 11, 2020. It was spread in almost all countries around the world rapidly [6]. As of April 26, 2023, the total number of people with COVID-19 infection has increased sharply to 686,676,972 confirmed cases, with 659,247,328 recovered and 6,860,939 deaths [7]. The most prevalent medical symptoms include hyperpyrexia, dry cough, breathlessness, malaise and myalgia [8]. Also, some patients may experience rhinorrhea, headache, chest pain, vomiting and diarrhea [9]. Organ function damages, such as acute respiratory distress syndrome, hyperglycemia, acute kidney injury, liver dysfunction, cardiac injury, etc., have been seen in most patients with COVID-19 [10]. According to previous studies, SARS-CoV-2 transmission rate is more significant than SARS-CoV, and its reason could be the enhanced transmission ability of SARS-CoV-2 following the rapid mutation and genetic recombination in the receptor-binding domain (RBD) region of the S protein. The structure of SARS-CoV-2 is the same as other coronaviruses with four structural proteins, spike (S), nucleocapsid (N), envelope (E) and membrane (M) proteins, such as helicase, 3-chymotrypsin-like protease, papain-like protease, RNA polymerase, etc. [11].

Numerous novel drug delivery systems (DDSs) have been proposed in recent years, such as stimuli-responsive DDSs, which achieve the accelerated/triggered release of therapeutic agents at the selective target site and improved cellular binding upon exposure to various external (light, heat, ultrasound and magnetic field) or internal (microenvironmental changes in pH, ROS and enzymes) stimuli. The stimuli-responsive DDSs may be classified as physical, chemical and biochemical stimuli-responsive, which are summarized in Fig. 1 [12].

Currently, a variety of nano-systems including nano-polymers, liposomes, micelles, dendrimers, carbon-based nanomaterials, nanogels and metallic nanoparticles are being used to create smart DDS that can respond to specific signals from their surroundings, whether they come from within the body or from the external environment [13]. Nanoparticles can be designed to have special surface properties. These properties help them only target and attack diseased cells, while leaving normal cells unharmed. This method makes drugs work better while reducing their adverse effects. Furthermore, nanoparticles can be made to release their cargo in a controlled manner, which means drugs can be released steadily over a long period of time. Nanoparticles offer several advantages, including small particle size, large surface area, and the ability to encapsulate drugs. These characteristics make them ideal candidates for designing stimuli-responsive drug delivery systems [14].

Stimuli-responsive materials can be designed to be biocompatible. They can be modified to exhibit different levels of responsiveness to different stimulators, which can be useful for future diagnostics and personalized medicine [13]. In addition, these materials exhibit observable or measurable changes at the nano or micro scale, such as molecular bonding rearrangement or cleavage, changes in morphology or molecular motion, leading to variations in macroscopic properties such as shape, color, and functionality. Due to their flexible range of functional groups and backbone structure, stimuli-responsive materials can be tailored to exhibit various chemical, mechanical, electrical, biological, optical or other properties. They also can be designed in different forms, including thin films, bulk materials, nano or microparticles, and composites [15]. Increasing pieces evidence have recently demonstrated the advantages of smart stimuli-responsive DDSs in treating a wide variety of diseases, such as cancers, diabetes, metabolic and Inflammation disorders [16–21]. This review provides insights into COVID-19 treatment by employing smart stimuli-responsive DDSs to potentiate the therapeutic effects of drugs and reduce their side effects. Stimuli-responsive DDS could be used for site-specific delivery and targeting of COVID-19-related health disruptions are summarized in Table 1.

## 2. Biochemical stimuli-responsive systems

### 2.1. *ROS-responsive*

Reactive oxygen species (ROS) is a biochemical term describing the small chemical molecules derived from oxygen molecules [35]. ROS mainly include oxygen free radicals, such as superoxide ($O_2^{\cdot -}$), peroxyl ($RO_2^{\cdot}$), hydroxyl ($\cdot OH$), and alkoxy radical ($RO^-$), as well as ozone ($O_3$), hypochlorite (HOCl), dioxidene ($^1O_2$), hypochlorite ($OCl^-$), and hydrogen peroxide ($H_2O_2$), which are not free radicals. These non-free radicals act as oxidants that can convert into radicals [36]. The ROS, which are released from immune cells such as dendritic cells, neutrophils and macrophages, plays essential roles in various biological functions of living organisms, like modifying protein functions, production of several hormones, regulation of cell signaling pathways and homeostasis, and mediation of inflammation [37]. Redox-responsive delivery systems offer several key benefits, including their ability to remain stable in contact with healthy tissues, thereby reducing the risk of systemic toxicity and unwanted side effects, which are observed in conventional pharmacotherapy. Additionally, they can quickly respond to elevated the levels of GSH concentration found in tumor cells, leading to the controlled release of therapeutic agents. Furthermore, they facilitate the targeted release of therapeutic agents within the cytoplasm, thereby enhancing the overall therapeutic efficacy [38].

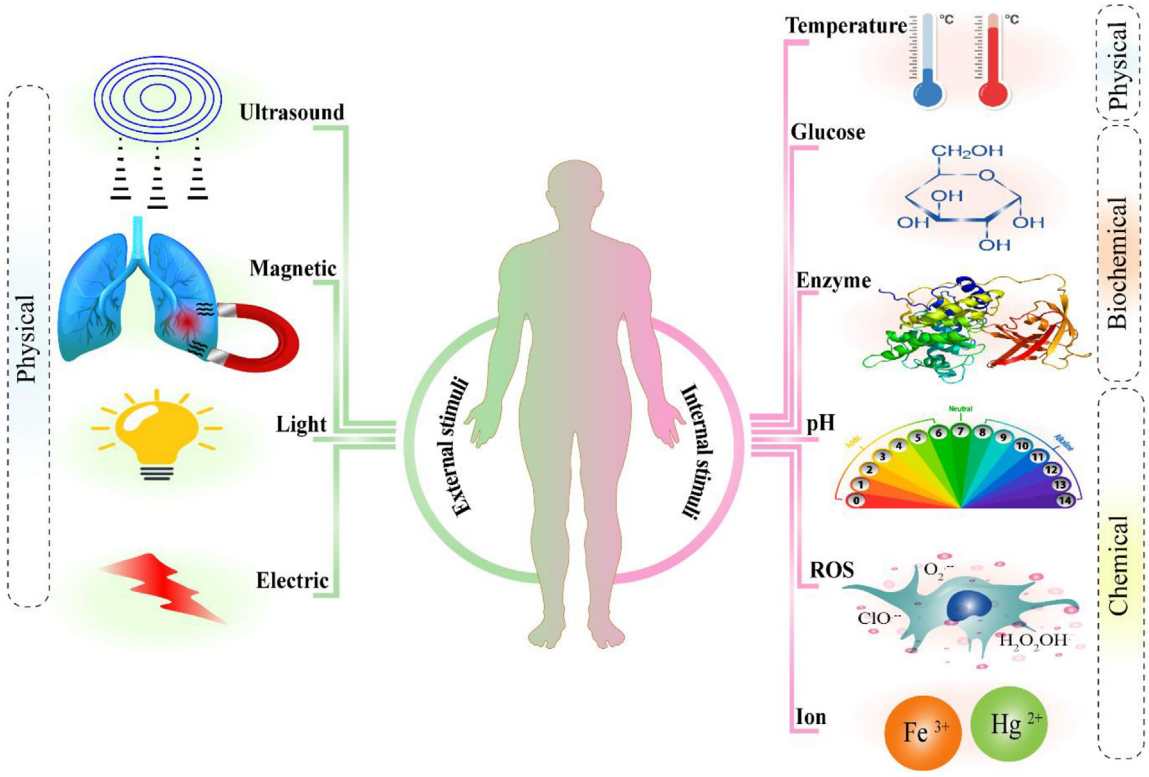


**Fig. 1 – Schematic diagram of classified smart stimuli-responsive drug delivery systemsystems and their activity and oxidation reaction mechanism.**

Environmental stress (*e.g.*, ionizing and UV radiation) [39] and some diseases, *e.g.* COVID-19, cancer, severe inflammatory diseases, etc. [40] can cause a significant imbalance between the production and removal of ROS. Its high concentration may result in apoptosis, severe pathological conditions, and oxidative stress (OS) damage to the cellular structures like; nucleic acids, lipids, carbohydrates and proteins [41].

COVID-19 infection, in severe cases, may cause a hyper inflammatory phase and oxidative stress in the infected tissues. Here, COVID-19-induced inflammation is a double-edged sword that may either protectively contribute to virus clearance and the patient's recovery process or deleteriously lead to the occurrence of acute respiratory distress syndrome (ARDS) and worsening of the disease [42]. From a pharmaceutical point of view, the implication of oxidative stress in severe COVID-19 could be used as a promising approach for targeted therapy. Therefore, DDSs can be designed to generate intelligent DDSs that respond to ROS stimuli in order to safely and efficiently deliver COVID-19 drugs, especially those with unstable and low bioavailability, to their therapeutic targets. In addition, some ROS-stimuli responsive systems can simultaneously suppress severe inflammation by scavenging ROS, contributing to inflammation, and releasing their cargo by selective transportation to damaged locations [43].

For example, Zhai et al. [22] prepared ROS-stimuli poly(1,4-phenyleneacetonedimethylene thioketal) and poly(thioketal urethane) copolymer nanoparticles containing dexamethasone acetate, in which the thioketal linkages can be cleaved by high levels of ROS in the lipopolysaccharide (LPS) induced-damaged lungs. The copolymeric nanoparticles could accumulate in the inflammatory lung sites and rapidly release the encapsulated cargo which leads to the reduction of the following: ROS levels, production of pro-inflammatory cytokines lung damage, and mortality in mice. Due to the anti-inflammatory and anti-oxidative synergistic effects, the prepared nanoparticles exerted more effectiveness than free dexamethasone acetate in treating LPS-damaged lungs. This approach can be very favorable in treating inflammation-related diseases such as COVID-19 [22]. Also, Li et al. [23] developed ROS-responsive nanoparticles (TPCD NPs) composed of tempol and pinacol esters of phenylboronic acid (PBAP) conjugated concurrently with $\beta$-cyclodextrin. Tempol, as the therapeutic agent, is a superoxide dismutase mimic molecule that can appropriately scavenge superoxide anions and oxygen radicals. Also, the PBAP group as a catalase mimic can eliminate hydrogen peroxide. Thus, TPCD is a broad-spectrum ROS scavenger and, the site-specific release of therapeutic agents from these nanoparticles is due to the oxidation-sensitive units of PBAP. *In vivo* evaluations of TPCD NPs have shown higher accumulation in the LPS-induced-damaged lung, lower production of IL-1$\beta$ and TNF-$\alpha$, and reduced OS compared to free tempol [23] (Fig. 2 and 3). Due to the anti-cytokine activity of tempol and its antioxidant features, it has been introduced as a candidate drug against COVID-19. Also, a double-blinded and randomized clinical trial (NCT04729595) studies its efficacy in COVID-19 [44]. Table 2 provides an overview of ROS-responsive groups in DDS.

**Table 1 – Stimuli-responsive drug delivery systems used for site-specific targeting of COVID-19-related drugs.**

| Types | Nature of carriers | System | Therapeutic agents | Study method | Result | Route | Ref |
|---|---|---|---|---|---|---|---|
| Biochemical | ROS-responsive | Polymeric NPs | Dex acetate | *In vitro/ In vivo* | Effective degradability properties upon exposure to ROS with low toxicity | i.v. | [22] |
| | | PBAP-CD NPs | Tempol | *In vitro/ In vivo* | Effective and safe treatment for oxidative stress-related diseases such as COVID-19 | i.d. | [23] |
| | Glucose-responsive | PBAP-based Hydrogel | Metformin | *In vitro/ In vivo* | Efficient stimuli-responsive release with the improvement of chronic inflammation | Intravertebral | [24] |
| | Enzyme-responsive | Polymeric conjugate | MTX | *In vitro/ In vivo* | localization of MTX and reduction of the total amount of drug administered and side effects | Intraarticular | [25] |
| | | PEG Hydrogel | Two HNE substrates | *In vitro* | An enzyme-responsive hydrogel platform to achieve tune release to the local environment | | [26] |
| Chemical | pH-responsive | Nanocomposites | Dex | *In vitro* | pH-sensitive system with significant improvement in cell viability compared to Dex alone | | [27] |
| | Ion-responsive | Polymeric Hydrogel | MTX | *In vitro/ In vivo* | Better therapeutic effect and fewer side effects | Intraarticular | [28] |
| Physical | Temperature-Responsive | Nanocapsules | Favipiravir | *In vitro* | Efficient thermo-responsive systems for the controlled release of hydrophobic medicines for the treatment of COVID-19 | | [29] |
| | | Polymeric antibody conjugate | | *In vitro* | a thermo-responsive polymer for increasing screening sensitivity | | [30] |
| | Ultrasound-responsive | Polymeric Microbubbles | MSC-Derived Exosomes | Simulation study | Rupture of polymeric microbubbles after US exposure to release cargo for treatment of lung injury | | [31] |
| | Magnetic-responsive | IO–NPs | | *In vitro* | Achieving non-toxic nanocarriers with promising candidates in the alternative treatment of COVID-19 | | [32] |
| | | MNPs-coated microcarriers | | In Silico | Improved drug delivery to different lobes of the lung by controlling the speed of entering the lung, the density of microcarriers and, the position of the magnetic field generator | | [33] |
| | | Zinc-MNPs | Montelukast | *In vitro* | Achieving targeted drug-carrying NPs with greater effectiveness than the free drug | | [34] |

NP: nanoparticle; PBAP: phenylboronic acid; HNE: human neutrophil elastase; CD: cyclodextrin; i.v.: intravenous; i.d.: intradermal; MSC: Mesenchymal Stem Cell; MTX: methotrexate; Dex: Dexamethasone.

### 2.2. *Glucose-responsive*

The smart glucose-responsive DDS can adjust the release of payload according to the change in blood glucose concentration. Typical glucose-responsive DDS are phenylboronic acid (PBA) and its derivatives, glucose-binding protein (*e.g.*, concanavalin A), and glucose oxidase [74]. Enzymes and proteins exhibit volatile inactivation, poor stability and high cost. However, PBA is a cost-effective and easy-to-fabrication-responsive synthetic polymer [75]. Glucose-responsive systems based on PBA capable of forming a reversible boronate group, and show a high affinity for cis-diol compounds. Its controlled drug release mechanism is through the contraction/expansion

**Table 2 – Overview of ROS-responsive groups in drug delivery systems and their activity and oxidation reaction mechanism.**

| ROS-responsive group | Chemical oxidation reaction | Mechanism of activity | Systems | Route | Ref |
|---|---|---|---|---|---|
| Selenium | 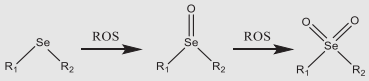 | Hydrophobic to hydrophilic phase transition | Micelle | *In vitro* | [45] |
| Diselenide | 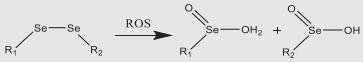 | Structural cleavage | Micelle | | [46] |
| thioether | 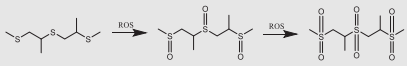 | Hydrophobic to hydrophilic phase transition | Nanocomplex, micellar NP, polymersome, hydrogel, microsphere | i.v., Intramuscular | [47–51] |
| vinyldithioether | 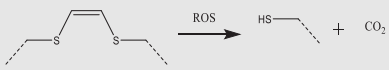 | Structural cleavage | Micelle | *In vitro* | [52] |
| Poly(thioketal) | 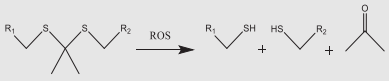 | Structural cleavage | Fibrous patch, polyplex, microsphere, NP | Transdermal, Oral, i.v. | [53–56] |
| Tellurium | 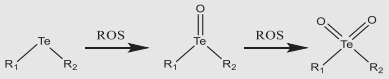 | Hydrophobic to hydrophilic phase transition | Micelle | | [57] |
| Arylboronic acid/esters | 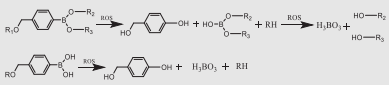 | Structural cleavage | Polyplex, NP, microparticle, micelle | Intraperitoneal, Ii.v. | [58–61] |
| polyoxalate | 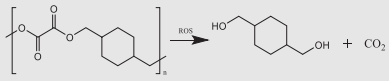 | Structural cleavage | Microparticle, NP | Intramuscular | [62,63] |
| Poly(L-proline) | 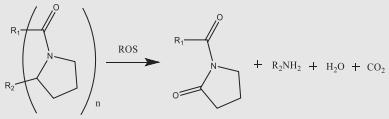 | Structural cleavage | Polymeric scaffolds | *In vitro* | [64] |
| Poly(L-methionine) | 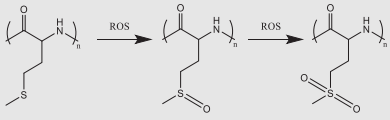 | Hydrophobic to hydrophilic phase transition | Vesicle | *In vitro* | [65] |
| Ferrocene | 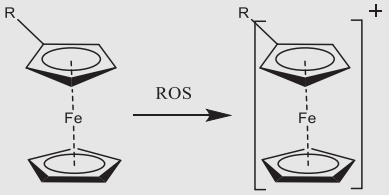 | Hydrophobic to hydrophilic phase transition | Micelle | *In vitro* | [66] |
| Polysaccharide | 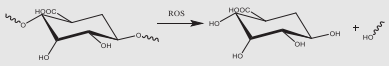 | Structural cleavage | NP | i.v. | [67] |
| Aminoacrylate | 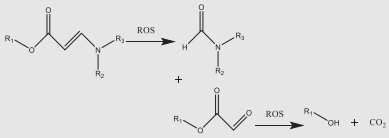 | Structural cleavage | NP | i.v. | [68] |
| HA | 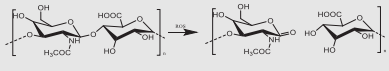 | Structural cleavage | NP | *In vitro* | [69] |
| Manganese oxide | 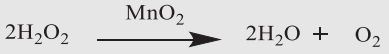 | – | Microparticle, NP | Transdermal, i.v. | [70,71] |
| Cerium | 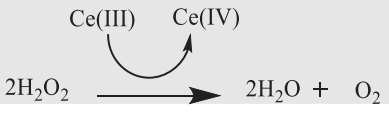 | – | NP | Transdermal | [72] |

(*continued on next page*)

**Table 2 (*continued*)**

| ROS-responsive group | Chemical oxidation reaction | Mechanism of activity | Systems | Route | Ref |
|---|---|---|---|---|---|
| Polylactic acid | 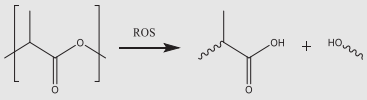 | Structural cleavage | NP | *In vitro* | [73] |

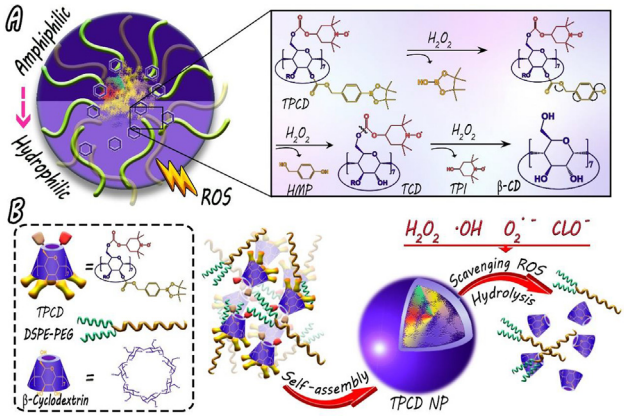


**Fig. 2 – A ROS-responsive nanoparticle for targeted treatment of acute lung injury. (A) The mechanism of self-immolative degradation in ROS-rich environments. (B) Schematic design of broad-spectrum ROS-scavenging nanoparticles. Redrawn from [23].**

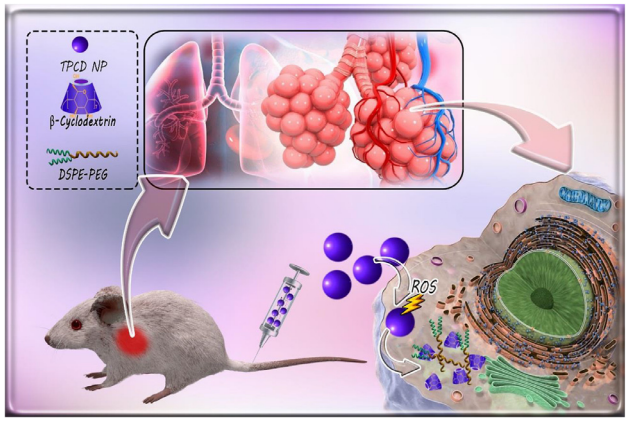


**Fig. 3 – Schematic representation of drug release process from ROS-responsive nanoparticles in acute lung injury mice model. Redrawn from [23].**

transfer of PBA or competitive reactions [76]. COVID-19 is a metabolic disease leading to hyperglycemia and other adverse outcomes. Hyperglycemia can lead to dysfunction of mitochondrial and activation of ROS production, increasing SARS-CoV-2 replication and proliferation, oxidative stress, inflammatory factors, and apoptosis induction. In several studies, hyperglycemia has been proven as a clear and robust poor prognostic factor in COVID-19. Compared to individuals without hyperglycemia, it can increase the risk of ARDS and mortality. Due to the high glucose uptake by viral-infected cells, such as those in COVID-19, glucose-responsive DDS offers targeted drug delivery to the sites of viral replication. This system uses glucose, which is a molecular trigger, to release the antiviral drug and ensures its safety and efficiency [77].

Zheng et al. [24] developed a PBA-based glucose-responsive system for metformin delivery (PBA-Met). Metformin, a therapeutic agent with anti-inflammatory and hypoglycemic effects, showed a controlled release in response to blood glucose concentration. PBA-Met improved the chronic inflammation caused by diabetes *in vivo* (Fig. 4). Therefore, by loading the appropriate drugs (hypoglycemic, anti-inflammatory, antiviral, etc.) in the smart glucose-responsive DDS, it is possible to control hyperglycemia and inflammation properly and, as a result, to improve COVID-19.

### 2.3. *Enzyme-responsive*

Acute pulmonary infection caused by the novel coronavirus disease in 2019 led to severe global health threats. Specific inflammatory microenvironmental stimuli can prompt smart DDS to release their cargo. One of the inflammatory biochemical stimuli is the overexpressed inflammatory enzymes [78]. Neutrophil elastase, cathepsins and MMPs are extracellular enzymes that are the most studied in designing responsive DDS in the case of inflammation [79]. Homma et al. [25] optimized hyaluronic acid (HA) and methotrexate (MTX) conjugates to serve as a polymeric prodrug with a cathepsin-cleavable peptide linkage (Phe-Phe chain). The optimized formulation inhibited human fibroblast-like synoviocytes from proliferating *in vitro*. It also inhibited knee swelling in rats with mono-arthritis induced by collagen.

Despite significant researches dedicated to enzyme-responsive DDSs, there are still certain issues that hinder their application in clinical. For example, the unique enzyme dysregulation in various stages of disease, whereas other diseases also exhibit an overexpression of certain enzymes [80]. Consequently, personalized enzyme-responsive DDSs need to be tailored based on the specific disease and its stage, while also considering the presence of other diseases in the patient. The second issue considers the liver and its role in clearing foreign substances and toxins. It contains a high concentration of hydrolases which may result in undesired drug release and systemic toxicity. Consequently, hydrolase-

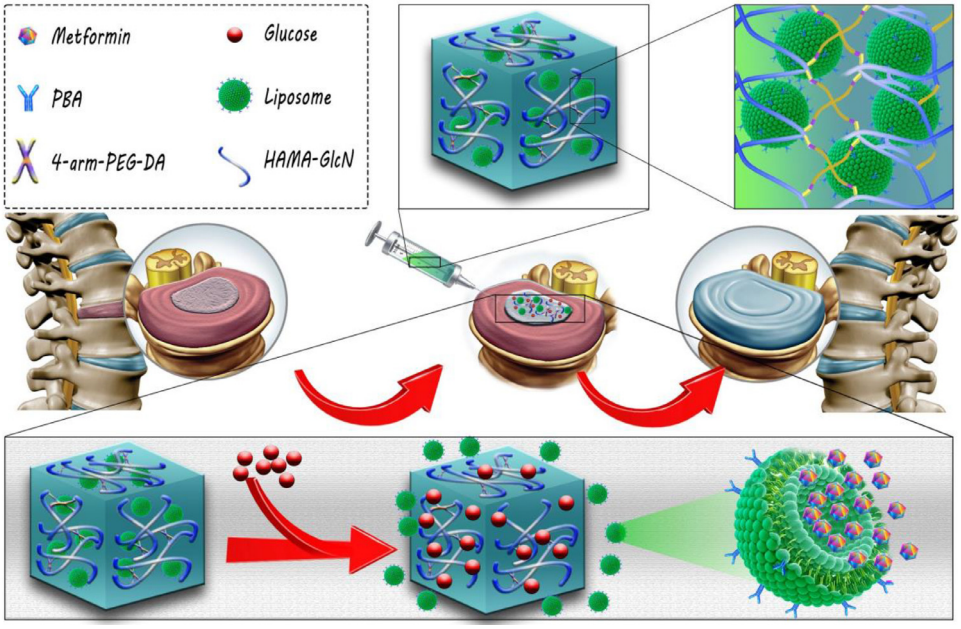


**Fig. 4 – Phenylboronic acid-based liposome containing metformin was loaded in the hydrogel consisting of 4-arm poly(ethylene glycol) diacrylate, hyaluronic acid (HA), methacrylic anhydride (MA) and D(+)-glucosamine hydrochloride (GlcN). When the glucose-responsive liposome-modified hydrogel was exposed to a high amount of glucose, metformin was released in the intervertebral space of rat model to create anti-inflammatory microenvironment and cause tissue regeneration. Redrawn from [24].**

responsive DDSs should be designed in a way to be protected from liver hydrolysis. Another novel enzyme-responsive DDS was designed by Aimetti and coworkers [26] to treat local inflammation. Neutrophils are the first cells attracted to inflammatory sites and secret a serine protease named human neutrophil elastase (HNE). Photopolymerization techniques were used to immobilize peptide linkers in polyethylene glycol (PEG) hydrogel. These peptide linkers, such as Ala-Ala-Pro-Val are sensitive to HNE. Therefore exposure to this elastase leads to the degradability of hydrogel *in vitro* (Fig. 5). These results show the great potential of enzyme-responsive systems to release their payloads in the site of action where the corresponding enzymes are overexpressed. (Table 3).

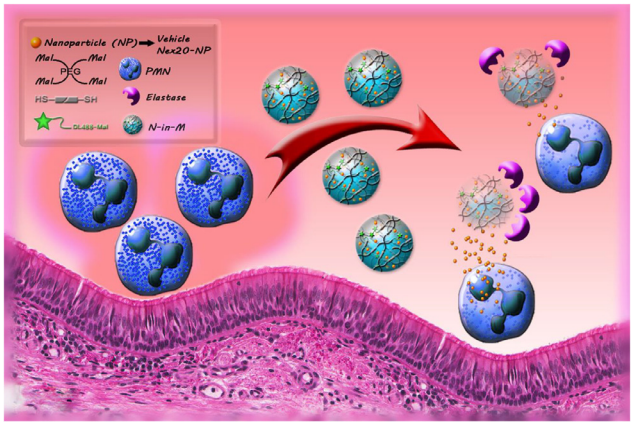


**Fig. 5 – Schematic representation of the drug release mechanism of Nexinhib20 (Nex20) from N-in-M (nanoparticles-in-microgel) elastase-responsive system in lung epithelium. Elastase enzyme increases following influx and continuous activation of polymorphonuclear neutrophils (PMN) in inflammation. The efficient delivery of Nex20 to the target site leads to significant systemic and lung inflammation blocking. SH, sulfhydryl; PEG, polyethylene glycol; MAL, maleimide. Redrawn from [26].**

## 3. Chemical stimuli-responsive systems

### 3.1. *pH-responsive*

Nanoparticles made of pH-responsive biomaterials have the potential to serve as DDSs and undergo deformation or disintegration when exposed to externally acidic or alkaline conditions. External pH conditions can modify intramolecular or intermolecular interactions of the pH-sensitive carriers and trigger the release of payloads [18,93]. There are two release mechanisms in pH-sensitive drug carriers: the first originates from changing in hydrophobicity or charge of carriers induced by protonation or deprotonation resulting from environmental pH variation, and the second is due to dynamic chemical bond cleavage in pH-sensitive biomaterials [93].

Despite several research efforts, there remain some limitations remain in the way of clinical translation of pH-responsive DDSs [94,95]. The stage and type of tumor effect on acidification of extracellular matrix ($pH_{ECM}$). This kind of heterogeneity in tumors makes challenge in designing DDSs that are activated by the tumor extracellular pH [96]. Also, the

**Table 3 – Classification of Overexpressed enzymes and illustrative examples of Enzyme-responsive nanoparticles with their characterization.**

| Enzymes | Sensitive sequences or moieties | Formulation forms | Therapeutic agents | Disease | Release mechanisms | Evaluation models/ Route of administration | Characterization | Ref |
|---|---|---|---|---|---|---|---|---|
| MMPs | TIMP | GST-TIMP-bFGF/collagen-GSH hydrogels | bFGF | MI | MMP-mediated hydrolysis of the substrate peptide between GST and bFGF | *In vitro* in HUVEC cells, *in vivo* in rats/ Intramyocardial | SEM, Rheometery, 1HNMR, FTIR, *in vitro* drug release, PCR, western Blotting, CCK-8 assay | [81] |
| | ppTAT | $PEG_2k$-ppTAT-$PEG_1k$-PE micelles | PTX | Various cancer cells | Cleaved by the active human MMP2 and $PEG_2k$ was deshielded thereafter | *In vitro* in A549, HeLa, HT1080MCF-7, NCI/ADR-RES and MDA-MB-231 cells; *in vivo* study in nude (BALB/c nu/nu) mice/ Intratumoral | 1HNMR, DLS, TEM, *In vitro* drug release, cellular uptake, CellTiter-Blue® Cell Viability Assay | [82] |
| Trypsin | FRFK | PASP-FRFK hydrogel | | | Triggered by the degradation of the hydrogel induced by trypsin; bulk erosion; surface erosion | *In vitro* in HepG2 cells | Gravimetric method to study the degradation of hydrogels, *in vitro* cytotoxicity, cytostatic activity and drug release | [83] |
| Neutrophil elastase | CGAAPVRGGGGC | N-in-M | Nex | Lung inflammation in ARDS, COPD and CF | NP release is triggered by enzyme cleavage activity, and the drug is released by passive diffusion | *In vitro* in Blood PMNs, *In vivo* in LPS-treated mice/ Intratracheal | *In vitro* transmigration experiments, Flow cytometry, EV analysis, Fluid assays | [84] |
| | K(ROX)AAPV ↓RGGGK(QXL) | PEGDA10k photopolymerized hydrogel | – | Inflammation | HNE dictates the release by entering the center of hydrogel and hydrolysis of its substrate | | 1H NMR, MALDI-MS, Enzyme Kinetic Analysis, confocal microscopy, Modeling enzymatic cleavage | [26] |
| Cathepsin D | FAAFFVLC | Graphene quantum dots | DOX | Cancer | Enzyme-triggered breakage of peptide linkages | *In vitro* in 4T1 cells, *in vivo* in mice/ i.v. | AFM, XPS, Cell cytotoxicity, CLSM, flow cytometry analysis | [85] |
| | Phe-Phe | Prodrugs | MTX | Osteoarthritis | Enzymatic cleavage of MTX | *In vitro* inhibition of the proliferation of human fibroblast-like synoviocytes, *in vivo* inhibition of the knee swelling of rats/ Intraarticular | 1H NMR, GPC analysis, Cathepsin fragmentation, LC–MS | [25] |
| Furin | GRVRRSC | Triterpenine-based liposomal complex (PEGcleavable Tf-CTM/L) | Tripterine | Cervical cancer | Passive diffusion; furin-cleavable PEG shell improves accumulation at the tumor site by steric hindrance | *In vitro* in HeLa cells, *in vivo* in Nude mice/ Intraperitoneal | DLS, TEM, *in vitro* drug release, flow cytometry, Cellular uptake, Cellular apoptosis, MTT assay, immunohistochemistry tests, CD-31 and a-SMA assay | [86] |

(*continued on next page*)

**Table 3 (*continued*)**

| Enzymes | Sensitive sequences or moieties | Formulation forms | Therapeutic agents | Disease | Release mechanisms | Evaluation models/ Route of administration | Characterization | Ref |
|---|---|---|---|---|---|---|---|---|
| | RVRRSK RX(K/R)RY | Graphene-based co-delivery nanocapsules | DOX and TRAIL | Cancer | TRAIL is released extracellularly by furin-associated cleavage, and DOX is released by acidity responsive | *In vitro* in A549 cells | AFM, *In vitro* release, CLSM | [87] |
| Protein kinase C$\alpha$ | FKKQGSFAKKK-$NH_2$ | Polymeric gene carriers consisting of PLL DNA polyplex | pDNA | Cancer | Intracellular PKC$\alpha$ phosphorylated the peptide and triggered the gene expression | *In vitro* in A549 cells, *in vivo* in male mice via the tail veins/ i.v. | $^1$H NMR, titration assay, DLS, Agarose gel electrophoresis, Cytotoxicity assay, Transfection study | [88] |
| | HFKKQGSFAKKK-NH2 | NPs | pDNA | Cancer | PKC$\alpha$ targeted the grafted cationic peptides and decreased their cationic charge, resulting in the release of pDNA from the polyplex | *In vitro* in B16 melanoma cells, *in vivo* in mice/ Microinjection | DLS, coupled enzyme assay, cytotoxicity test, microinjection study, Transfection study, western blotting assay | [89] |
| Caspase-3 | DEVD (Asp-Glu-Val-Asp) | NPs | DOX | Breast cancer | NIR-triggered PDT, then the activated enzyme cleavage DOX prodrug | *In vitro* in MCF-7 and 4T1 cells, *in vivo* in female mice/ i.v. | DLS, TEM, $^1$H NMR, flow Cytometry, CLSM, FCM, Western Blotting Analysis, Cytotoxicity Assays | [90] |
| | AGVA | Nanocapsules | Caspase-3 protein | Cancer | Upon proteolytic cleavage of the cross-linker, the polymeric shell Disintegrated and the protein is released | *In vitro* in HeLa cells | DLS, TEM, cytotoxicity assay, Bright-field-microscopy | [91] |
| MPO | Luminol | NPs | LCD | Inflammation | Degradation of NP under oxidative conditions and enzyme-triggered hydrolysis of NPs | *In vitro* in neutrophils and macrophages, *in vivo* in mice/ Intraperitoneal | FTIR, DLS, TEM, SEM, Cellular uptake, Fluorescence images, migration test | [92] |

TIMP: MMP-2/9 cleavable peptide PLGLAG; MI: myocardial infarction; ppTAT: MMP2-cleavable peptide (GPLGIAGQYGRKKRRQRRRC); PTX: paclitaxel; FRFK: a tetrapeptide, composed of phenylalanine (Phe, F), arginine (Arg, R) and lysine (Lys, K); PASP: poly(aspartic acid); CGAAPVRGGGGC: a di-sulfhydryl elastase peptide; N-in-M: NP-in-microgel containing a backbone with NE-degradable peptide; Nex: Nexinhib20, a potent neutrophil degranulation inhibitor; ARDS: acute respiratory distress syndrome; COPD: chronic obstructive pulmonary disease; CF: cystic fibrosis; TRAIL: membrane-associated cytokine; PEGDA10k: Poly (ethylene glycol) Diacrylate; AFM: atomic force microscopy; XPS: X-ray photoelectron spectroscopy; FAAFFVLC: Phe-Ala- Ala-Phe-Phe-Val-Leu-Cys; GRVRRSC (G: glycine; R: arginine; V: valine; S: serine; C: cysteine); RVRRSK RX(K/R)RY (R: arginine; K: lysine; X: any amino acid; Y: the cleavage site); PLL: poly-L-lysine; pDNA: plasmid DNA; PDT: photodynamic therapy; LCD: luminol-conjugated $\beta$-cyclodextrin.

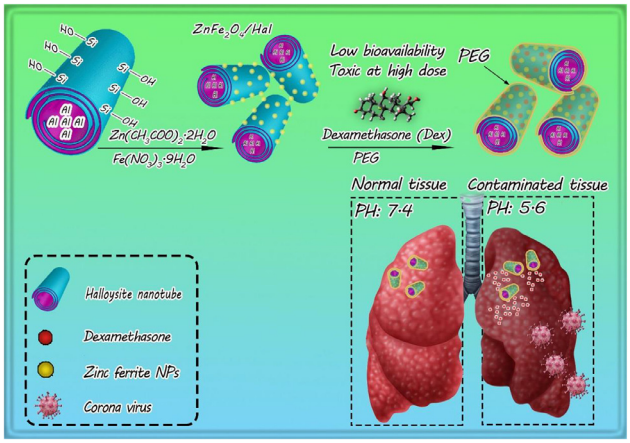


**Fig. 6 – Representation of the structure and preparation method of PEGylated ZnFe2O4/Hal nanocomposite with pH-sensitive release of Dex under infected lung pH of 5.6 and neutral pH of 7.4. Redrawn from [27].**

$pH_{ECM}$ can vary within the same tumor depending on tumor volume. When drugs are delivered to specific parts of the body with lower acidity levels, like certain cells, nanocarriers should be internalized by endocytosis to trigger drug release. However, they are needed to escape from the endosomes, otherwise the drug will be degraded by the acidic condition and enzymes of the lysosomes.

It is essential to consider targeting strategies in order to prevent possible systemic toxicity due to the low pH found within inflammation lesions. The attachment and entry of SARS-CoV-2 into the affected cells is pH dependent and happens at pH 5.5. Jermy et al. [27] developed a halloysite (Hal) nanoformulation and compared the release capability of dexamethasone (Dex) under infected lung pH condition and neutral pH (5.6 vs 7.4) (Fig. 6). Hal ($Al_2Si_2O_5$ $(OH_4)\cdot 2H_2O$) is a mineral of natural clay like kaolin with the intrinsic ability of drug release in response to pH variations. A small amount of Dex (less than 5%) was released at neutral pH, while it was released 17.5% at pH 5.6 in a sustained manner. The sustained release may be attributed to the differences in charge distribution between the internal and external surfaces of nanotubes. Si-O-Si groups on the exterior surface are negatively charged, while the lumen part is aluminum-rich and positively charged. Hydroxyl groups of Dex interact with active sites of Hal. PEG was used to coat over Dex nanocomposites. This coating protects normal cells from the toxic side effects of Dex until it reaches the infected tissue [27,97]. These results suggest that pH-sensitive materials have high stability and huge potential to prevent the premature release of drugs, making them a promising pulmonary drug delivery platform for targeting lung infections in patients suffering from COVID-19. (Table 4).

### 3.2. *Ion-responsive*

Nitric oxide (NO) is one of the critical biomarkers in many diseases. It is an unstable gas that quickly turns into stable products, including nitrate and nitrite. Low NO concentration *in vivo* has reduced the sensitivity of NO-responsive DDSs. The higher concentration of nitrite ($NO_2^-$) than NO has led to the evolution of $NO_2^-$-responsive DDS for treating NO-related diseases [108]. Previous studies have reported that the C–C binding of 4′ in dihydropyridine compounds reacts with the nitrosyl ion generated from $NO_2^-$, thus being selectively cleaved via oxidative aromatization. If cross-linkers are created in the DDS with dihydropyridine derivatives, breaking these linkers will lead to the collapse of the hydrogel and smartly release the loaded drug [109]. In a study, Xiong et al. [28] synthesized a $NO_2^-$ responsive polyacrylamide hydrogel with a dihydropyridine cross-linker. Methotrexate was loaded into the hydrogel and used for inflammatory arthritis treatment (Fig. 7). The *in vitro* and *in vivo* findings have shown that a portion of the polymeric hydrogel was decomposed according to the concentration of $NO_2^-$ and released methotrexate. The release of methotrexate inhibited inflammation, reduced the concentration of $NO_2^-$ and stopped the decomposition of the hydrogel. The smart $NO_2^-$-responsive hydrogel could reduce adverse effects caused by methotrexate overdose and maintain long-acting therapeutic efficacy [28].

In moderate to severe COVID-19 patients, hyper inflammation and increased blood levels of nitrate and nitrite compared to healthy people require rapid drug release with a sufficient dose to relieve symptoms in time [110]. Also, drug delivery should be stopped when the symptoms are resolved to avoid long-term unwanted side effects and drug overdose. Therefore, a $NO_2^-$-responsive DDS can be an ideal treatment with better therapeutic outcomes and fewer side effects for COVID-19 than traditional treatments.

## 4. Physical stimuli-responsive systems

### 4.1. *Temperature-Responsive*

Thermo-responsive DDSs have received more attention among stimuli-responsive systems, and have mostly been tested for anticancer drugs and imaging agents, as shown in Table 5 [17]. Temperature can be external (light irradiation/heating from outside and magnetic/ electric fields) or internal (due to infection). The solubility of thermo-responsive systems changes in response to the temperature. Thermo-responsive nanostructures have several advantages: low toxicity and high specificity [111]. Although there are benefits, some major drawback limits the applicability of thermo-responsive DDSs. The main issue is controlling the temperature for many materials in one DDS. It is important to set the temperature higher than normal body temperature to prevent premature releasing of the cargo. This high temperature needs an external heat source. However, most of the time, we cannot clearly define the exact temperature at which a response occurs. Instead, we only notice a gradual change in the patterns of release as the temperature increases. As a result, it becomes impossible to have precise control over the release temperature. Tumor temperature might not always be hotter than the normal surrounding tissues, and even sometimes tumors may have lower temperature. On the other hand, when there is inflammation

**Table 4 – Categories of pH-responsive delivery systems with example polymers and release descriptions.**

| Category | Polymers | Polymer type | Formulation type | Model drug | Route | Mechanism | Ref |
|---|---|---|---|---|---|---|---|
| Anionic | P(MAA-g-EG) | Synthetic | Microgel | OVA | Oral | NPs are encapsulated in the microgels in acidic conditions and protected in the stomach (pH 1–3), then released in the neutral pH of the small intestine (pH 5–8) | [98] |
| Cationic | DC–Cholesterol•HCl | Synthetic | Lip | DOX | | Acidic pH can elevate cationic and fusogenic features of DC-liposomes, then electrostatic interactions happen via an anionic endosomal membrane, which causes endosomal escape | [99] |
| Amphiphilic | mPEG-b-PCHGE | Synthetic | Micelles | PTX | i.v. | Polymeric micelles are degraded in low pH because of containing an acetal group as a pH-responsive cleavable linkage | [100] |
| Degrading polymer | Ge/SA based polymeric composites | Natural | Hydrogel | CTZ | | Maximum swelling was at pH 1.2, and the release of drug occurred through non-Fickian diffusion or anomalous mechanism. | [101] |
| Polyanion | Eudragit® L100-Based | Synthetic | Nanofiber | NIC | | Polymer is disintegrated at pH values higher than 6 and used for targeted drug delivery to the colon. | [102] |
| Polycation | Chitosan-Based | Natural | NP | Cab | i.v. | Drug is released continuously under the acidic TME because chitosan has pH-triggered degradability | [103] |
| Polycation | Apt conjugated chitosan | Bio-synthetic | NP | 5FU & DOX | | Acidic pH-induced protonation in the -$NH_2$ group of chitosan and increased drug release. | [104] |
| Polyanion & polycation | PBAE and NaAlg | Synthetic and natural | Lip-polymer HNP | Spe | i.v. | Tertiary amine residues in PBAE were protonated in acidic pH, which caused swelling of NPs and rapid drug release | [105] |
| Inorganic material | Mesoporous Carbon | Synthetic | NP | DOX | S.C. | Polymer can inhibit release at pH 7.4, which shows the *in vivo* biosafety. But the polymer is disassembled at pH 5 and drug releases in a sustained manner. | [106] |
| Other | PAAm-g-XG | Synthetic | NP | Cur | Oral | Optimum release was in pH 6.8, due to the ionization of –COOH groups and electrostatic repulsion of the ionized groups, which produce micropores and increase drug release | [107] |

P(MAA-g-EG): poly(methacrylic acid) with PEG; OVA: ovalbumin; 3ß-[N-(N',N'-dimethylaminoethane)-carbamoyl]cholesterol hydrochloride: DC-Cholesterol•HCl; Lip: liposom; mPEG-b-PCHGE: poly(ethylene glycol)-block-poly(cyclohexyloxy ethyl glycidyl ether)s; PTX: paclitaxel; Ge/SA: gelatin/sodium alginate; CTZ: Cetirizine; NIC: niclosamide; Cab: Cabazitaxel; Apt: aptamer; 5FU: 5-fluorouracil; DOX: doxorubicin; HNP: hybrid nanoparticle; PBAE: polycationic polymer poly($\beta$-amino ester); NaAlg: polyanionic sodium alginate; Spe: Spectinomycin; S.C.:Subcutaneous; PAAm-g-XG: polyacrylamide-grafted-xanthan gum; Cur: Curcumin.

in the body, the tissues affected can be warmer than usual. This may cause drugs to be released in the wrong place from temperature sensitive DDS. As a result, depending solely on endogenous stimuli for temperature changes has some restrictions, and creating exogenous temperature-responsive DDS has proven to be more effective [112].

Xu et al. [29] loaded favipiravir in nano capsules with a polymer coating and subsequently incorporated them in layer-by-layer self-assembled films. Poly (methacrylic acid) (PMAA) homopolymers were used in multilayer film structures and displayed swelling/de-swelling behaviors under temperature stimulus. The multilayer films covered by poly(N-isopropylacrylamide)-b-poly(N,N-dimethylaminoethyl methacrylate) (PNIPAM-b-PDMAEMA) block copolymers, and these coronae caused steric hindrance and layering distance during film growth. PNIPAM collapsed above its lower critical solution temperature (LCST) and lost water resulting in strong hydrophobic–hydrophobic interactions between favipiravir and coronae, thus decreasing drug diffusion. At lower environmental temperatures, PNIPAM chains were hydrated and hydrophobic–hydrophobic interactions were weakened. This kind of swelling leads

**Table 5 – Examples of temperature-responsive and multi-temperature-responsive nanocarriers used in DDS.**

| Formulation | Polymer used | Disease | Drug | Preparation method | Characterization | Route | Refs |
|---|---|---|---|---|---|---|---|
| **Thermo-responsive** | | | | | | | |
| Liposomes | DPPC, DSPE-PEG, monoalkyl phospholipids | Prostate cancer | DOX | Extrusion method | DLS Zeta-potential, DSC | *In vitro* | [113] |
| Cationic Liposome | DPPC, DC–Chol, DOAB, Chol, $Fe_3O_4$, Ammonium sulfate | Cervical Cancer | OXA and MDC1-AS | Decompression evaporation, Extrusion | TEM, DLS, Electrophoretic mobility, laser particle size analysis | i.v. | [114] |
| Injectable thermosensitive PNT-gel | PPG-peg, $\alpha$-CD | Breast cancer | DOX | Oxidative polymerization, host-guest self-assembly | FTIR, H NMR, TGA, UV–vis-NIR absorption spectra, XRD, Rheological test, Real-time thermal images, fe SEM, MALDI-TOF-MS | Intratumoral | [115] |
| Biodegradable NPs | PNIPAAm, chitosan, TPP | Prostate Cancer | Cur | Free radical polymerization, PNIPAAM-COOH was grafted onto chitosan using EDC/NHS as the condensing agent | FTIR, LCST analysis, DLS, Zeta potential measurements, TG/DTA, DTG, XRD, SEM | *In vitro* | [116] |
| Thermogel | PLGA-PEG-PLGA (1800–1500–1800) | Ophthalmic drug delivery model | RhB, C 6 | were purchased | *In vivo* study | Subconjunctival | [117] |
| Liposomes | DPPC, DSPE-PEG2000, MSPC | Glioma tumor | DOX | Dissolution | Fluorescent imaging | i.v. | [118] |
| *In situ* gels | P407, HPMC, MC | Glaucoma | BH | Dispersion under continuous stirring | Test tube inversion method, Gelling capacity test | Ocular | [119] |
| Supramolecular vesicle (temperature-responsive nanoenzyme) | Ad-NIPAM, CD-Se | Oxidative damage | —- | Polymerization (in Schlenk tube equipped with a magnetic bar and an oil bath followed by three freeze–pump–thaw cycles), | H NMR, MALDI-TOF, ESI-MS and GPC, SEM, TEM, UV–vis spectroscopy, LCST | —- | [120] |
| Cationic liposomes | DPPC, DSPC, $DPPG_2$ or DSPE-PEG2000, DPTAP | Solid Tumors | DOX | lipid film hydration and extrusion method | DLS, DSC | i.v. | [121] |
| Liposomes | DPPC, DSPE-PEG2000, MSPC | Human lung large cell carcinoma | F7 and TPT | lipid film hydration and extrusion | DLS, TEM, DSC | i.v. | [122] |
| Artificial Extracellular Matrix | HA, PNIPAM | Tissue engineering | — | Graft polymerization | H NMR, GPC with HPLC, Static contact angle by sessile drop method | | [123] |
| Nanoaggregate | Chitosan, Pluronic | Hydrophobic drug delivery | IMC | Graft polymerization | CAC, hydrodynamic size, and surface morphology by fluorescence spectroscopy, DLS, TEM | *In vitro* | [124] |
| Nanoparticles | NIPAAm, MAA | Breast cancer | Cur | Free radical mechanism | FTIR, H NMR, SEM | *In vitro* | [125] |
| Nanocomposite Hydrogels | ZnO, PNIPAm | Anti-mold property | — | Radical polymerization method | FTIR, TEM, DSC, DLS | *In vitro* | [126] |
| Nanohybrid hydrogels | Chitosan/ Graphene | Breast cancer | MTX | Mixing | FTIR, XRD, SEM | *In vitro* | [127] |

(*continued on next page*)

**Table 5 (*continued*)**

| Formulation | Polymer used | Disease | Drug | Preparation method | Characterization | Route | Refs |
|---|---|---|---|---|---|---|---|
| Injectable hydrogel | Trimethyl chitosan/ tripolyphosphate | Anemia | EPO | — | DLS, SEM, digital rotary | S.C. | [128] |
| **Thermo-and pH-responsive** | | | | | | | |
| Smart nanogel system | PNIPAM | Breast cancer | ANST | Solvent evaporation technique | FTIR, DSC, XRD, TEM, AFM, DLS, optical spectroscopy, | *In vitro* | [129] |
| Nanohydrogels | Lactoferrin conjugated PNIPAM-acrylic acid (LF-PNIPAM-co-AA) | Breast cancer | HK | Graft copolymerization, free radical polymerization, carbodiimide coupling reaction, | FTIR, zeta potential experiments, H NMR, MALDI TOF-MS analysis, LCST analysis, DSC, XRD, TEM, DLS, SEM | i.v. | [130] |
| **Temperature/pH/Enzyme Triple-Responsive** | | | | | | | |
| hydrogels | PLGA-PEG-PLGA, CS, SeNP | Hepatocellular carcinoma | SOR | Ring-opening polymerization, emulsification and solvent evaporation technique | NMR, FTIR, Raman Spectroscopy, DLS, TEM, Rheological analysis, XRD, H NMR, | Intratumoral | [131] |
| Nanogel | Protamine/PAA-b-PNIPAAm | Breast cancer | DOX | radical polymerization method, directly heating | FTIR, NMR, GPC, Zeta potential measurement, LCST analysis by UV/Visible spectrophotometer, | *In vitro* | [132] |

OXA: oxaliplatin; MTCL: magnetic thermosensitive cationic liposome; PNT-gel: photothermal-network hydrogel; PPG-peg: PEGylated poly(N-phenylglycine); Cur: Curcumin; BH: betaxolol hydrochloride; TPT: topotecan; RhB: Rhodamine B, C6: coumarin 6; IMC: Indomethacin; HK: Honokiol; SOR: sorafenib; EPO: erythropoietin; ANST: anastrozole;.

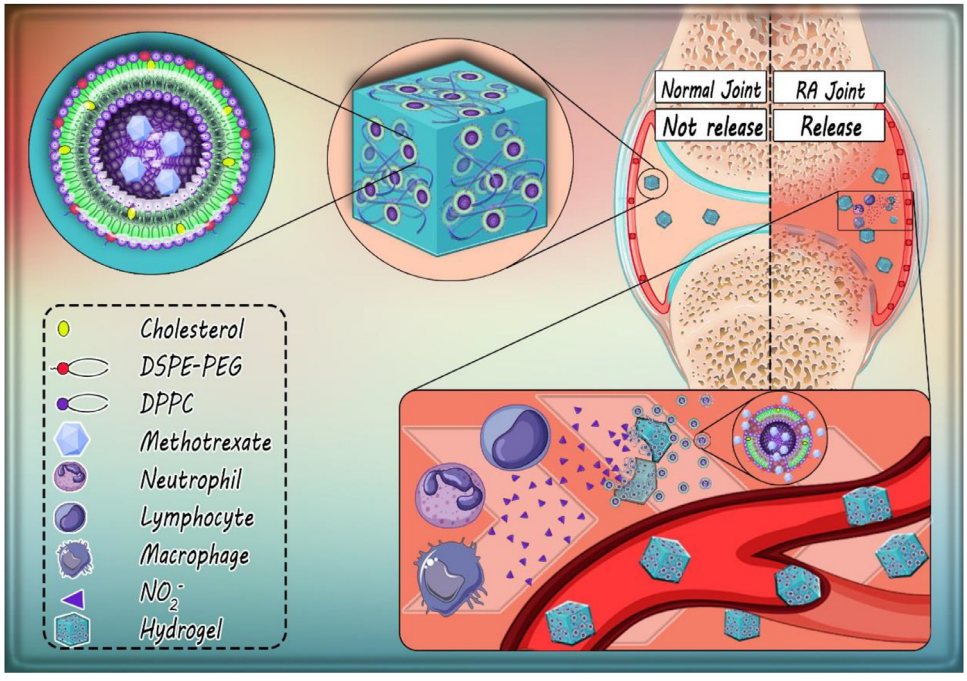


**Fig. 7 – Schematic illustration of methotrexate liposome loaded in nitrite (NO2-)-responsive hydrogel (DHPL-GEL), degradation in the rheumatoid arthritis (RA) rat model due to nitrite produced following the activity of over-activated immunological cells and drug release process. Redrawn from [28].**

to drug diffusion as it loses the network structure of the block copolymer. So, the drug release was consequently temperature-dependent and increased as the temperature dropped.

Also, Nabil et al. [30] synthesized a temperature-responsive polymer based on poly (N-isopropylacrylamide-co-2-hydroxyisopropylacrylamide-co-strained alkyne isopropylacrylamide) continued by conjugation with the antibody of SARS-CoV-2. These polymeric antibody conjugates increased the recombinant protein samples of SARS-CoV-2 nucleocapsid around six-fold, reducing the misdiagnosis of patients in immunoassay tests as the viral load increased. PNIPAAm is one of the temperature-responsive polymers with an LCST of 32 °C. Below 32 °C, hydrophilic amides of the PNIPAAm bond with water molecules. These water molecules surround the hydrophobic parts of PNIPAAm, including isopropyl groups, resulting in complete water solubility. In opposition, above LCST, PNIPAAm hydration turns to an unstable state and leads to dehydration and aggregation of polymers because of hydrophobic interactions. So the water solubility of PNIPAAm can be easily controlled by temperature [30]. Therefore, temperature-responsive materials can be a promising agent for diagnostic purposes and treatment of current endemic COVID-19.

### 4.2. *Ultrasound-responsive*

Ultrasound technology is one of the most common promising physical agents in diagnosis, increasing drug/gene delivery efficiency and therapeutic efficacy of various drugs. Ultrasound waves have attracted increasing attention due to their relatively low cost, portability of ultrasound tools, non-invasive technique, non-ionizing nature, safety, and deep penetration into tissue and living cells. In drug/gene delivery systems, ultrasound precisely controls encapsulated drugs' spatial and temporal release, while minimizing their systemic effects [133]. Despite the positive aspects, there are still some issues that need attention in order for ultrasound-responsive DDSs to be suitable for clinical applications. The optimal size of nanocarriers should be under 250 nm to take advantage of EPR effect and prevent rapid clearance during circulation. Conversely, achieving high sonosensitivity becomes challenging with small particle size and compact nanostructure. While the addition of sonosensitive materials can enhance nanocarriers' response to ultrasound, it may negatively affect the stability of the DDSs and reduce their circulation half-life [94]. In addition to the sonosensitivity issues, ultrasound cannot pass through air-filled areas, and ultrasound-responsive drug delivery systems are not suitable for tumors located externally or surrounded by organs like the lungs and bowels. Another drawback is the need for MRI guidance to optimize therapeutic efficiency, and these combined ultrasound-MRI systems are sophisticated and costly [134].

Recently, scientific works have been significantly devoted to optimizing different types of vehicles, such as microbubbles, nanobubbles, micelles and nanoliposomes. Most microbubbles, the well-known ultrasound-responsive materials, are composed of phospholipid, polymer or protein outer shells and gaseous cores; and have a size of about 1-10 μm. In the ultrasound treatment process, these microbubbles encapsulated with the drug are injected into the bloodstream. However, until exposure to ultrasound waves, the interaction of the encapsulated drug with the surrounding environment is prevented; then, the ultrasound is focused on the desired specific area and causes the microbubbles to release the drug, which is absorbed by the surrounding tissues [135]. Recent studies have shown that exosomes and mesenchymal stem cells can be beneficial for repairing and treating lung damage caused by viral infections. Also, in moderate to severe COVID-19 patients who were treated with mesenchymal stem cells and exosomes derived from them, the efficacy of the treatment was shown in the form of immune modulation, improvement of pulmonary function, and reduction of cytokine levels [136]. Therefore, Fonseca et al. [31] evaluated the efficiency of the ultrasound signals required to penetrate tissue layers reaching alveoli containing polymeric microbubbles loaded with mesenchymal stem cell-derived exosomes (Fig. 8). The results showed that ultrasound-based therapy combined with mesenchymal stem cell-derived exosomes could be used for immediate treatment of patients with lung injury and recovered patients who may suffer from recurrent viral infection. Microbubbles remain inactive until they are exposed to ultrasound signals. Upon exposure to low-frequency ultrasound waves (*i.e.*, 0.1 MHz regardless of ultrasound intensity), they release their loaded cargo through rupture and oscillation [31]. As a result, ultrasound-mediated controlled drug delivery of microbubbles can help treat COVID-19 patients, especially in targeting the heterogeneously damaged pulmonary endothelium that current therapies cannot target [137]. Table 6 summarizes ultrasonic-responsive materials in DDS and their ultrasound frequency.

### 4.3. *Magnetic-responsive*

Magnetic systems are mainly used for imaging and controlled drug release. Magnetic nanoparticles (MNPs) have an easy synthesis method (including co-precipitation or microemulsion), large specific surface area, and small particle size, and are also biodegradable and biocompatible. All the mentioned characteristics have made MNPs recognized as a potential DDS. However, certain issues need to be resolved in order to facilitate their clinical development. First, adding MNPs to temperature-responsive DDSs helps to solve the problem of the clumping particles together. However, this approach may reduce the strength of magnetism and restrict the effectiveness of the DDSs because the MNPs are covered by an external material [158]. Secondly, the use of a large amount of magnetic materials and exposure to high-frequency alternating magnetic fields (AMF)when using magneto-responsive DDSs can cause heart problems and damage to the peripheral nervous system and spinal cord, even if non-toxic carriers are used [95]. Thirdly, the application of alternating magnetic force in an appropriate arrangement is challenging and costly for cancer metastasis and deep-seated tissues. However, when the desired location is well-defined, magnetically responsive DDSs can be a suitable option [159].

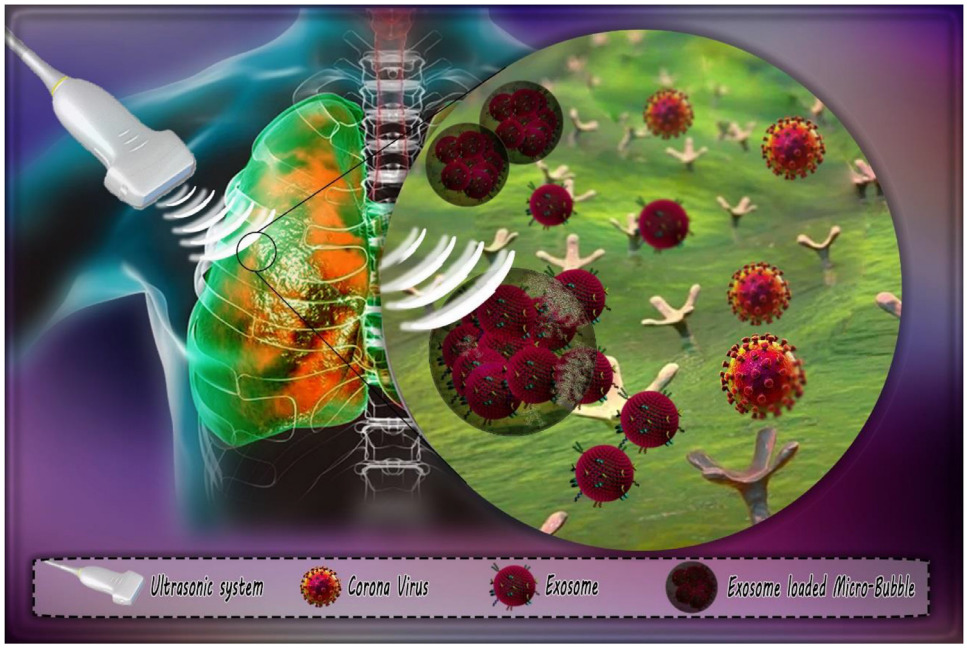


**Fig. 8 – Schematic illustration of ultrasound-responsive polymeric microbubble containing exosome in treating lung injury of COVID-19. Ultrasound signals break the microbubbles, and exosomes are released in the lung infected with the coronavirus. Redrawn from [31].**

Several studies have shown the effectiveness of iron oxide nanoparticles (IO–NPs) in preventing the pathogenicity of coronaviruses and different types of influenza viruses with the mechanism of physical attachment to the envelope and spike protein subunits of the SARS-CoV-2, changing their structure and thus inactivating the virus [160]. For example, Martins et al. [32] prepared $Fe_3O_4$ nanoparticles by co-precipitation, and then obtained DMSA-$Fe_3O_4$ thiolated nanoparticles through coated by meso–2,3-dimercaptosuccinic acid (DMSA). Their cellular results did not show any toxicity in the cells of COVID-19 patients and healthy people. Also, due to free thiol groups of DMSA, all types of proteins and/or drugs used in the remedy of COVID-19 can benefit from targeted drug delivery that is responsive to the magnetic system by covalently binding to DMSA-$Fe_3O_4$ nanoparticles. The nanoparticles play their role in preventing virus binding to host cells and serve as carriers for a protein/drug (Fig. 9) [32].

Also, Ebrahimi et al. [33] investigated targeted drug delivery to the lung lobes treating COVID-19 patients using microcarriers coated with magnetic nanoparticles *in silico* study. The performance of drug delivery to different lung branches is affected by various factors, including the rate of lung penetration, the density of microparticles, and the position of the magnetic field generator. In this study, the whole lung has been divided into four main lobes, including the right lower lobe (RLL), left lower lobe (LLL), right upper lobe (RUL) and left upper lobe (LUL). The best drug delivery performance to the LUL and LLL lobes was observed by positioning the magnetic field generator at an angle of ~30°. Also, a significant increase in drug delivery to the lung was shown by changing the input speed from constant to pulsatile. Micro carrier adhesion to LLL and RLL lobes showed a direct relationship with the increase in inlet velocity. In contrast, the maximum adhesion for LUL and RUL lobes was observed at an inlet velocity of ~0.574 m/s. Microcarriers with high and low density caused the best drug delivery to the lower and upper lobes, respectively [33]. Therefore, it is suggested to promote the use of MNPs as a beneficial treatment for the endemic of COVID-19.

### 4.4. *Light-responsive*

Light is desirable as one of the external and physical stimuli that include a broad spectrum of waves such as ultraviolet (UV), visible (Vis) and near-infrared (NIR). The main advantages of light-responsive DDSs are cost-effectiveness, target-specificity, tissue position adjustability, precise control of light intensity and frequency, duration of exposure, and non-invasiveness. Despite their speed, convenience and accuracy, light-responsive DDSs have numerous drawbacks that restrict their application in clinical settings, including: (1) DDSs that are responsive to light usually rely on UV or Vis light to either break bonds or produce ROS. However, both of these light sources have limited ability to penetrate tissues. Additionally, UV poses safety risks as it can damage nucleic acids [161]; (2) NIR-based DDSs have been developed, demonstrating enhanced penetration below the skin by up to 10 cm and reduced side effects. However, the presence of biological components along the light pathway can strongly absorb NIR [162]; (3) Thorough assessment of the biocompatibility, long-term safety, and biodegradability of materials that can respond to a two-photon adsorption effect is necessary, as they typically have a lower energy barrier, demonstrate aggregation-induced emission energy conversion behaviors, initiate photo-induced

**Table 6 – Summary of ultrasound-responsive materials in drug delivery systems and their ultrasound frequency.**

| Ultrasound-responsive core | Chemical formula | Shell material | Delivery system | Ultrasonic frequency | Route | Ref |
|---|---|---|---|---|---|---|
| Calcium carbonate | $CaCO_3$ | PEG-b-poly(L-aspartic acid) | Polymeric nanobubble | 40 MHz | Intratumoral | [138] |
| Oxygen | $O_2$ | Sodium CMC | Polymeric nanobubble | 40 MHz | Intravesical | [139] |
| 1% Carbon dioxide | $CO_2$ | Protein | nanobubble | 18 MHz | i.v. | [140] |
| Tetrafluoromethane | $CF_4$ | Poly lactide-co-glycolide | Polymeric nanobubble | 1 MHz | i.v. | [141] |
| Perfluoropropane | $C_3F_8$ | Herceptin-PEG-DPPE- DSPC-DSPE | Nanobubble | 5–12 MHz | i.v. | [142] |
| | | DPPC-DPPA | Nanobubble | 1.3 MHz | *In vitro* | [143] |
| | | Folate-conjugated N-palmitoyl chitosan | Nanobubble | 7 MHz | i.v. | [144] |
| | | Mix DSPC, DSPE-PEG2000 and DSPE-PEG2000-biotin | Nanobubble | 1 MHz | *In vitro* | [145] |
| | | PLA-PEG-NH2 | Nanobubble | 9 MHz | *In vitro* | [146] |
| | | Herceptin-PEG-PLGA | Nanobubble | 1, 40 MHz | *In vitro* | [147] |
| Perfluoropentane | $C_5F_{12}$ | RGD modified poly(methacrylic acid/Glycine/PEG | Nanobubble | | i.v. | [148] |
| | | Poly lactide-co-glycolide | Droplet | 1 MHz | i.v. | [149] |
| | | Perylene diimide | Droplet | 40 MHz | i.v. | [150] |
| | | POPE, POPC, cholesterol, and DSPE-PEG-2000 | Droplet | 2 MHz | S.C. | [151] |
| 2H,3H-decafluoropentane | $C_5H_2F_{10}$ | Chitosan-lecithin | Polymeric nanobubble | 3 MHz | *In vitro* | [152] |
| Perfluorohexane | $C_6F_{14}$ | Phosphatidyl ethanolamine | Droplet | 1 MHz | i.v. | [153] |
| | | O-carboxymethyl chitosan | Droplet | 9 MHz | *In vitro* | [154] |
| | | Polydopamine | Droplet | 7.5 MHz | *In vitro* | [155] |
| Perfluoroheptane | $C_7F_{16}$ | Pluronic F68 | Droplet | 2.5 MHz | *In vitro* | [156] |
| Perfluorononane | $C_9F_{20}$ | DSPC and mPEG-DSPE | Droplet | 2.25 MHz | *Ex vivo* | [157] |

chemical reactions, serve as photosensitizer (PS), and have complex chemical composition. [163]; (4) Certain types of light-responsive medications can raise safety concerns because they require several minutes of intense exposure to light. Furthermore, when the NIR light penetrates deep into tissues up to 10 cm beneath the skin, the biological components along that path absorb the NIR light [164].

The activation mechanism of light-responsive DDSs can be classified into five general categories: photolysis, photopolymerization, photoisomerization, photo-redox and photothermal (Fig. 10) [165]. Photolysis causes the disintegration of the DDS structure by breaking the light-responsive linkers (such as o-nitrobenzyl) at a specific wavelength of light in the polymer and other materials, so the drug is released at the target site. The presence of unsaturated bonds in some light-responsive materials causes cross-linking, shrinkage of the DDS, and the creation of a pore through which drug release occurs. In photoisomerization, the density packing of the bilayer carrier is disturbed and drug release is caused by changing the configuration from Trans to Cis following light irradiation. The photo-redox mechanism (the relevant mechanism in photodynamic therapy) leads to structural changes in lipids and the creation of new electric charges by producing ROS species. Finally, the drug release occurs by creating pores and micelles in the bilayer carrier. In the photothermal mechanism, the light-responsive material generates heat through light radiation. As a result, the body responds to the temperature increase in that area, which can induce ROS species and cause drug release [166]. The most common light-responsive materials, according to their release mechanisms, are summarized in Table 7.

UV light has been used to activate PS in surface tissues. However, Vis and NIR lights have been used in deep body tissues [167]. Antimicrobial photodynamic therapy (APDT) has recently emerged as an alternative tool in treating various diseases, including viral infections. The antiviral action of APDT is that the PS can target nucleic acids, lipids and proteins of the virus by passing through the outer layer of the virus and producing ROS following the irradiation of blue laser light [168]. The study of Pourhajibagher et al. [169] has shown the anti-COVID-19 activity of APDT (10% wt curcumin-poly (lactide-co-glycolide) nanoparticles (Cur@PLG-NPs) as PS

**Table 7 – The most common light-responsive materials.**

| Mechanism | Light-responsive group | Light-responsive material | System | Wavelength (nm) | Route | Ref |
|---|---|---|---|---|---|---|
| Photolysis | o-nitrobenzyl | PEG-star-2-(4-nitro-3-benzyl carbonate camptothecin) phenoxyethyl methacrylate | Silver NPs | 365 | *In vitro* | [175] |
| | | S-(o-Nitro-m–methoxy-pazide Alkoxy Benzyl Ester) | Polymeric NPs | 980 | i.v. | [176] |
| | Pyrene methyl ester | 4-oxo-4-(pyrene-4-ylmethoxy) butanoic acid | Mesoporous silica NPs | 980 | *In vitro* | [177] |
| | Coumarin | Dicyanomethylene-coumarin | Small-molecule NPs | 505 | i.v. | [178] |
| | | [7-(diethylamino)coumarin-4-yl]methyl | Block copolymer | 794, 365 | | [179] |
| | | 6–bromo-7-hydroxycoumarin-4-ylmethyl | Polymeric micelles | 794 | | [180] |
| | Ru complex | Ru complex | Mesoporous silica NPs | 974 | *In vitro* | [181] |
| | Benzoin | Benzoin heptanoic ester | Polyester NPs | 355 | | [182] |
| | Bis(3-triethoxysilylpropyl) disulfide | Mesoporous organosilica-Bis(3-triethoxysilylpropyl)disulfide | Mesoporous silica nanogates | 760 | *In vitro* | [183] |
| Photopolymerization | Diacetylenic (1,2-bis(trideca-12-ynoyl)-sn-glycero-3-phosphocholine) | 1,2 bis(tricosa-10,12-diynoyl)-sn-glycero-3-phospho-choline | Liposome | 254 | | [184] |
| | Coumarin dimers | Coumarin dimers | – | >310 | | [185] |
| photoisomerization | Azobenzene | Azobenzene containing poly($\varepsilon$-caprolactone) chains | Supramolecular polymer | 365 | *In vitro* | [186] |
| | | monoacylated azobenzene ($AzoC_{10}N^+$) | Liposome | 350–450 | *In vitro* | [187] |
| | Spiropyran | Poly(acrylic acid-*co*-spiropyran methacrylate) | Nanogel | 520 | *In vitro* | [188] |
| | | Spiropyran | Block copolymer | 365 | *In vitro* | [189] |
| | | 1′-(2-hydroxyethyl)−3′,3′-dimethyl-6-nitrospiro(2H1-benzopyran-2,2′-indoline) | Polymeric micelle | 365 | *In vitro* | [190] |
| Photo-redox | Curcumin | Curcumin | Polymeric NPs | 450 | *In vitro* | [169] |
| | Methylene blue | Methylene blue | – | 630–808 | Transdermal | [191] |
| | | Methylene blue-Radachlorin | – | 662 | *In vitro* | [170] |
| | Phthalocyanine | Aluminum tetrasulfophthalocyanine hydroxide (AlPcS40H) | – | 780 | | [192] |
| | Indocyanine green | Poly(propylene sulfide)-Indocyanine Green | Polymeric micelles | 808 | i.v. | [193] |
| | | Diselenide-indocyanine green | Hydrogel | 808 | *In vitro* | [194] |
| | | Diselenide- indocyanine green | Polymeric micelles | 808 | *In vitro* | [195] |
| | | Indocyanine green | – | 780 | | [196] |
| Photothermal | Polydopamine | Polydopamine film-$NH_4HCO_3$ | Nanobomb | 808 | i.v. | [197] |
| | | Polydopamine-gold NPs | Hydrogel | 780 | i.v. | [198] |
| | IR780 | IR780-loaded polymeric micelle | Micelle | 808 | i.v. | [199] |

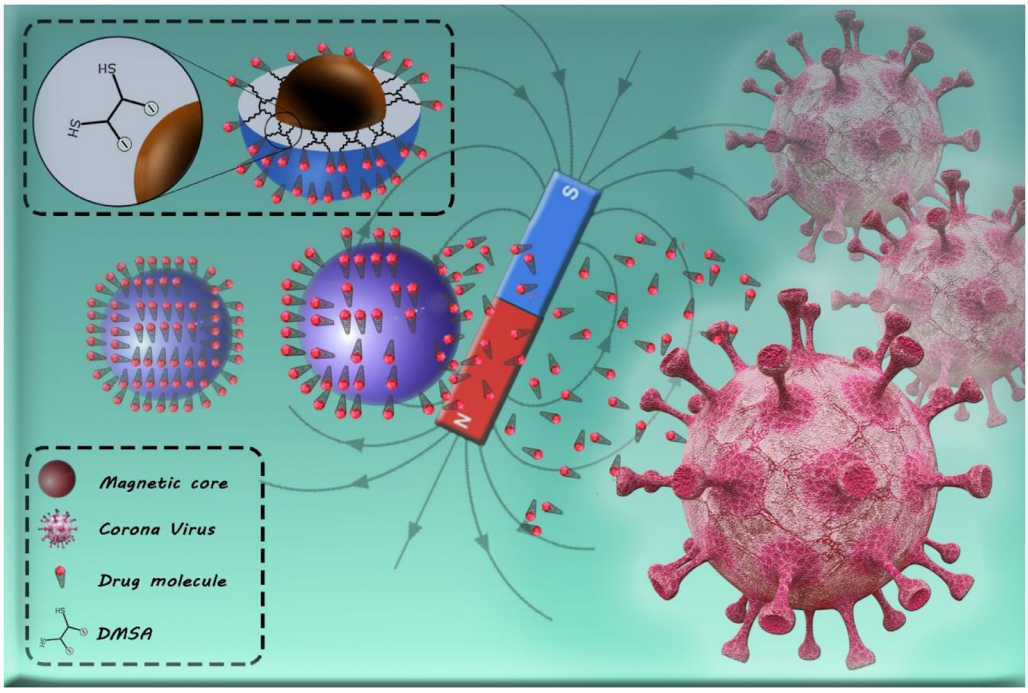


**Fig. 9 – Design and potential use of iron oxide nanoparticles containing meso–2,3-dimercaptosuccinic acid (DMSA) molecule as a magnetic drug delivery platform against COVID-19 disease. Redrawn from [32].**

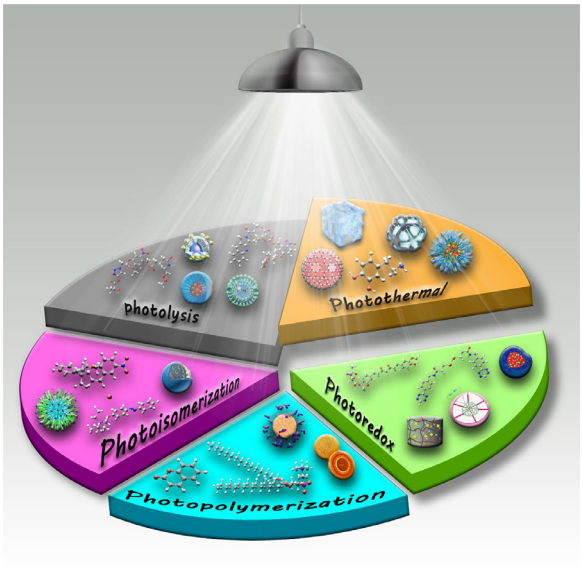


**Fig. 10 – Schematic illustration of light-responsive drug delivery systems and their activation mechanisms, including photolysis, photopolymerization, photoisomerization, photoredox and photothermal.**

combined with blue light at 5.228 MJ/m$^2$) *in vitro* on Vero cells treated with SARS-CoV-2-enriched plasma. The APDT did not show cytotoxic effects, while cytotoxic effects were observed by treating cells with Cur@PLG-NPs or lonely light. Therefore, it is possible to improve and accelerate the effectiveness of treatment in a controlled and targeted manner by loading anti-COVID-19 drugs into nanoparticles.

Several studies have described the occurrence of orofacial lesions related to COVID-19. Since photobiomodulation therapy (PBMT) and APDT can be used to inactivate the virus, reduce inflammation, reduce pain, and repair tissue in these lesions associated with COVID-19 [170], Sachet et al. [171] investigated the therapeutic results of PBMT/APDT methods. Since these lesions are caused by SARS-CoV-2, it is better to initiate APDT during the first 1–2 d of treatment. Subsequently, PBMT should be continued until complete recovery. In this study, the complete recovery of the patients was achieved within 12 d after applying light radiation in 660-808 nm. Also, a study has reported the success of PDT in disinfecting COVID-19 patients' nasal and oral cavities during the early stages of the disease [172].

Methylene blue (MB) is one of the ideal PS for APDT, which has direct virucidal effects on various viruses, including Ebola, MERS-CoV and SARS-CoV-2, even without activation by light irradiation [173]. The antiviral mechanism of MB in COVID-19 involves inhibiting the ACE2 receptor and SARS-CoV-2 spike protein. Unlike antibiotics, MB-mediated APDT can be an appropriate therapy for COVID-19 patients with secondary infections without developing resistance [174].

### 4.5. *Electric-responsive*

The field that surrounds electrically charged particles is known as the electric field. The flow of electrons through conductive materials creates an electric current. Organisms are affected by electric currents in various ways, from cellular to molecular levels. For instance, exposure to pulsed electric

**Table 8 – Conducting polymers used in stimuli-responsive drug delivery systems.**

| Conductive polymer | Formulation type | Polymer | Drug | Therapeutic use | Route | Ref |
|---|---|---|---|---|---|---|
| Polyaniline | Hydrogel | CP Hydrogel | Amo and Ibu | Antibacterial conductive hydrogel for precise dosing of medicine | S.C. | [205] |
| | Nanofibrous scaffold | Polylactide/ Polyaniline | – | Promoting osteogenic differentiation | *In vitro* | [206] |
| Polypyrrole | Micelle | SDBS | Dex | Drug delivery to different ranges of disease states | *In vitro* | [207] |
| PEDOT | Electrode Coating/ Film | SNPs | Melatonin Dox | Tissue engineering scaffolds, and drug delivery systems | Transdermal | [208] |
| Natural derivatives | Hydrogel | CMC | 5FU | Electrically controlled non-ionic drug delivery | Transdermal | [209] |

SNP: Sulfonate-modified nanoparticle; SDBS: Sodium dodecyl benzene sulfonate; Dox: Doxorubicin; CMC: carboxymethyl cellulose; PEDOT: Poly(3,4-ethylenedioxythiophene); CP: Chitosan-graft-polyaniline; Amo: Amoxicillin; Ibu: Ibuprofen; 5FU: 5-fluorouracil.

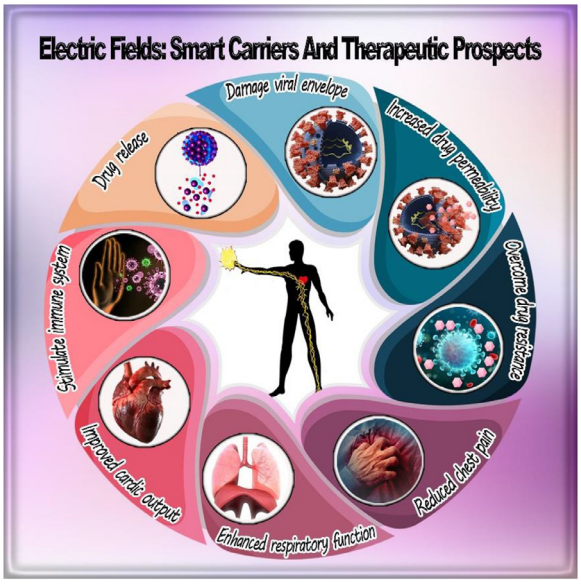


**Fig. 11 – Electric stimulus with two benefits on COVID-19 patients: (1) Therapeutic effects on COVID-19 symptoms including decreased chest pain, improved cardiac output, increased respiratory function and, etc.; (2) Triggering drug release in electric-responsive nanocarriers.**

field resulted in membrane pores formation and signaling pathway disturbance [200]. According to the literature review, electric stimulation can reduce the viral burden and be a practical approach in COVID-19 patients. Also, electric current can increase drug penetration. As reported by Kumagai et al., HIV1 was damaged by 1-min exposure to 1 volt of direct electric current. Destruction of HIV1 (in MAGIC-5 cells) could result from electrical stimulation on the envelope and cell membrane of the virus,thereby inhibiting the virus entry into cells. It is worth mentioning that electric stimulus is safe for normal cells as it does not cause any damage to host cells (MAGIC-5 cells) compared to viruses [201]. Furthermore, Kolsek et al. reported the effectiveness of electric current treating Herpes zoster (HZ) [202]. These preclinical pieces of evidence show the possibility of antiviral effects of electric current.

This strategy may also have therapeutic benefits for COVID-19 patients, such as reducing chest pain and facilitating breathing by stimulating the collapsed alveolar tissues to opened normal. Additionally, the electric stimulus can refine cardiac output by instigating cardiac muscles [203]. Furthermore, it can boost immunity and induce anti-inflammatory effects by regulating the expression of T&B cells and inhibiting the systemic rise in pro-inflammatory cytokines. Also, the growth of SARS-CoV-2 can be inhibited by electric stimulation. Viruses can be affected by electric currents through different mechanisms. For example, ROS species have antiviral activity as well as antibacterial activity. Previous studies have reported that 5 min exposure to 1 volt of electric stimulation increases ROS and NO species levels [203].

Electric-responsive materials, such as conductive polymers, release their therapeutic cargo in response to electric excitation. Conductive polymers containing ionic and electronic materials undergo volumetric expansion/ contraction due to electrochemical oxidation/reduction in an electrolyte. Synthetic conductive materials include polypyrrole, polythiophene, sulfonated styrene, polyvinyl alcohol and polyaniline, while chitosan, alginate and hyaluronic acid are the natural ones [204]. Table 8 summarizes some electro-responsive DDSs and their releasing mechanisms.

Altogether, these findings suggest that application of electrical stimulus-based treatment to COVID-19 patients may be a promising adjuvant therapy, which could also have synergistic effects when combined with electric-responsive materials as DDSs (Fig. 11).

## 5. Conclusion and future perspectives

The outbreak of COVID-19 prompted a global investigation into rapid and cost-effective technologies for the diagnosis,

prophylaxis and treatment. Despite this, the multiple mutations of SARS-CoV-2 has posed many challenges in developing these emerging technologies. Significant advances have been achieved in developing DDSs up to now. Stimuli-responsive DDSs have been shown to improve therapeutic efficacy and reduce side effects by releasing antiviral drugs particularly on the target site, in response to different internal/external stimuli. Various microenvironmental changes or biochemical signals associated with COVID-19 infection, including low pH, increased ROS, overexpressed enzymes, hypoxia, increased body temperature, etc., trigger the release of therapeutic molecules in the targeted area. As mentioned earlier, the different pathological characteristics of COVID-19 can be used in the design of delivery systems to target lungs and other organs affected by SARS-CoV-2. Additionally, the pathological conditions can be used for the evolution of targeted systems. For example, leaky vasculature results in passive accumulation, active targeting with ligands specific for over-expressed epitopes and platforms that are sensitive to internal triggers like pH, temperature, redox species, and so on.

Regardless of these developments, there are very few investigations of stimuli-responsive DDSs in animal models. Some critical challenges should be mentioned. First, the optimal stimuli should be selected according to the particular characteristics of the disease. The level of local acidosis varies among different inflammatory disease. In addition, normal organs and organelles with acidic environments such as the stomach and endolysosomes may cause undesirable drug release from pH-responsive drug carriers. Moreover, the type of inflammatory disease and different stages of similar disease may result in different amounts of ROS production or the dominant type of ROS. Enzyme-responsive systems could also be affected since some enzymes are expressed in non-target other tissues, leading to off-target drug release. Therefore, these issues complicate and limit the design and formulation of stimuli-responsive systems. Second, preparation procedures of currently available stimuli-responsive DDSs need to be optimized in order to obtain reasonable results, including clearly defined material structures, adjustable physicochemical features, and good reproducibility. Economic scale-up is also a key factor ensuring clinical advantages and low cost, which is critical for managing pandemic diseases. Third, new *in vivo* models with similar pathophysiological conditions of human diseases are required to be developed and utilized pre-clinically. Up until now, most studies on stimuli-responsive DDSs have been investigated in murine models. Therefore, the obtained results cannot be directly applied to humans due to these significant differences. The last point is the importance of acute and chronic toxicity evaluations of stimuli-responsive materials/systems. They should exhibit maximum drug efficacy while minimizing side effects in order to provide patients with therapeutic benefits that outweigh potential risks.

Nanotechnology has transformed the healthcare industry, leading to the investigation of innovative drug products known as nanomedicines. Stimuli-responsive DDSs belong to the category of nanoparticulate systems. However, the approval process for these nanotherapeutic products has been slow and challenging, with only a few successfully transitioning from development to clinical use. Nanoparticle-based DDSs are complex constructs with various components that confer unique properties, such as targeting specific sites or protecting labile drugs in the body. Designing these constructs requires precision, extensive characterization, and an understanding of the spatial arrangement of the components. Additionally, manufacturing large batches and ensuring consistency are essential. Developing nanomedicines differs significantly from conventional drug development and requires revised approaches to product design, chemistry, manufacturing, and quality assurance. K Key considerations for nanomedicine development include understanding the individual components and their interactions, identifying critical attributes, establishing quality control parameters, using validated assays for characterization, achieving sterility, targeting desired sites, ensuring stability, efficacy, safety, and product half-life. Nanomaterial-based medicines are highly complex and require precise design to ensure consistent quality. The Quality by Design approach is recommended, emphasizing understanding the product, process, and critical quality attributes based on scientific rationale and risk assessment. Nanoparticles' physicochemical properties and biological performance depend on factors such as size, surface charge, shape, coating, and drug release kinetics. Different nanomaterials (*e.g.*, liposomes, proteins, inorganic materials) have unique properties and synthetic procedures; therefore a tailored approach is necessary. Overall, developing nanotherapeutic products requires addressing the challenges associated with each nanoparticle independently [210,211]. Due to several challenges in the way of clinical translation, only very few systems have reached clinical development, especially for cancer therapy. Future research efforts in developing nanosystems that are highly sensitive to distinct variations in specific stimulus may lead to a greater number of stimuli-responsive DDSs to reaching the clinic.

However, despite the mentioned drawbacks, a few stimuli-responsive systems have reached clinical development in the case of cancer therapy. For example, ThermoDox® is the first thermosensitive formulation of doxorubicin-loaded liposomes that is utilized in human clinical trials [212]. Currently, ThermoDox® is in phase II/III of clinical trials for breast cancer and hepatocellular carcinoma. Opaxio® is another formulation entering phase III clinical trials as a potential treatment for ovarian cancer [213]. In Opaxio®, paclitaxel is conjugated to a biodegradable polyglutamate polymer, which is metabolized by lysosomal enzyme like cathepsin B. This metabolism facilitates the release of drugs and results in tumor cell suppression [214]. The iron oxide NanoTherm® AS1 has been approved by the European Union regulatory for then treatment of glioblastoma. This can be stimulated by the application of an alternating magnetic field from an external source. As mentioned above, studies have demonstrated the successful translation of stimuli-responsive carriers from preclinical models to clinical trials, future research efforts may lead to promising results in COVID-19 therapy.

## Conflict of interest

The authors declare no conflict of interest.

## Acknowledgements

The authors acknowledge the financial support of Isfahan University of Medical Sciences by grant No.#199180.

REFERENCES

[1] Zhong N, Zheng B, Li Y, Poon L, Xie Z, Chan K, et al. Epidemiology and cause of severe acute respiratory syndrome (SARS) in Guangdong, People's Republic of China, in February, 2003. Lancet 2003;362(9393):1353–8.
[2] van Boheemen S, de Graaf M, Lauber C, Bestebroer TM, Raj VS, Zaki AM, et al. Genomic characterization of a newly discovered coronavirus associated with acute respiratory distress syndrome in humans. MBio 2012;3(6):e00473 -12.
[3] Raj VS, Mou H, Smits SL, Dekkers DH, Müller MA, Dijkman R, et al. Dipeptidyl peptidase 4 is a functional receptor for the emerging human coronavirus-EMC. Nature 2013;495(7440):251–4.
[4] Dijkman R, Jebbink MF, Gaunt E, Rossen JW, Templeton KE, Kuijpers TW, et al. The dominance of human coronavirus OC43 and NL63 infections in infants. J Clin Virol 2012;53(2):135–9.
[5] Chen Y, Liu Q, Guo D. Emerging coronaviruses: genome structure, replication, and pathogenesis. J Med Virol 2020;92(4):418–23.
[6] Jiang S, Du L, Shi Z. An emerging coronavirus causing pneumonia outbreak in Wuhan, China: calling for developing therapeutic and prophylactic strategies. Emerg Microbes Infect 2020;9(1):275–7.
[7] Available from https://www.worldometers.info/coronavirus/.
[8] Zu ZY, Di Jiang M, Xu PP, Chen W, Ni QQ, Lu GM, et al. Coronavirus disease 2019 (COVID-19): a perspective from China. Radiology 2020;296(2):E15–25.
[9] Petrosillo N, Viceconte G, Ergonul O, Ippolito G, Petersen E. COVID-19, SARS and MERS: are they closely related? Clin Microbiol Infect 2020;26(6):729–34.
[10] Lu JQ, Lu JY, Wang W, Liu Y, Buczek A, Fleysher R, et al. Clinical predictors of acute cardiac injury and normalization of troponin after hospital discharge from COVID-19. EBioMedicine 2022;76:103821.
[11] Gorkhali R, Koirala P, Rijal S, Mainali A, Baral A, Bhattarai HK. Structure and function of major SARS-CoV-2 and SARS-CoV proteins. Bioinform Biol Insights 2021;15:11779322211025876.
[12] Zhao Y, Guo Y, Tang L. Engineering cancer vaccines using stimuli-responsive biomaterials. Nano Res 2018;11(10):5355–71.
[13] Badeau BA, DeForest CA. Programming stimuli-responsive behavior into biomaterials. Annu Rev Biomed Eng 2019;21:241–65.
[14] Yusuf A, Almotairy ARZ, Henidi H, Alshehri OY, Aldughaim MS. Nanoparticles as drug delivery systems: a review of the implication of nanoparticles' physicochemical properties on responses in biological systems. Polymers 2023;15(7):1596.
[15] Khizar S, Zine N, Errachid A, Elaissari A. Introduction to stimuli-responsive materials and their biomedical applications. In: Nazarzadeh Zare E, Makvandi P, editors. Stimuli-responsive materials for biomedical applications. ACS Publications; 2023. p. 1–30.
[16] Yang G, Song J, Zhang J. Biomimetic and bioresponsive nanotherapies for inflammatory vascular diseases. Nanomedicine 2020;15(20):1917–21.
[17] Mura S, Nicolas J, Couvreur P. Stimuli-responsive nanocarriers for drug delivery. Nat Mater 2013;12(11):991–1003.
[18] Lu Y, Aimetti AA, Langer R, Gu Z. Bioresponsive materials. Nat Rev Mater 2016;2(1):1–17.
[19] Saravanakumar G, Kim J, Kim WJ. Reactive-oxygen-species-responsive drug delivery systems: promises and challenges. Adv Sci 2017;4(1):1600124.
[20] Fu X, Hosta-Rigau L, Chandrawati R, Cui J. Multi-stimuli-responsive polymer particles, films, and hydrogels for drug delivery. Chem 2018;4(9):2084–107.
[21] Rajkovic O, Gourmel C, d'Arcy R, Wong R, Rajkovic I, Tirelli N, et al. Reactive oxygen species-responsive nanoparticles for the treatment of ischemic stroke. Adv Ther 2019;2(7):1900038.
[22] Zhai Z, Ouyang W, Yao Y, Zhang Y, Zhang H, Xu F, et al. Dexamethasone-loaded ROS-responsive poly (thioketal) nanoparticles suppress inflammation and oxidative stress of acute lung injury. Bioact Mater 2022;14:430–42.
[23] Li L, Guo J, Wang Y, Xiong X, Tao H, Li J, et al. A broad-spectrum ROS-eliminating material for prevention of inflammation and drug-induced organ toxicity. Adv Sci 2018;5(10):1800781.
[24] Zheng D, Chen W, Ruan H, Cai Z, Chen X, Chen T, et al. Metformin-hydrogel with glucose responsiveness for chronic inflammatory suppression. Chem Eng J 2022;428:131064.
[25] Homma A, Sato H, Tamura T, Okamachi A, Emura T, Ishizawa T, et al. Synthesis and optimization of hyaluronic acid–methotrexate conjugates to maximize benefit in the treatment of osteoarthritis. Bioorg Med Chem 2010;18(3):1062–75.
[26] Aimetti AA, Tibbitt MW, Anseth KS. Human neutrophil elastase responsive delivery from poly (ethylene glycol) hydrogels. Biomacromolecules 2009;10(6):1484–9.
[27] Jermy BR, Ravinayagam V, Almohazey D, Alamoudi W, Dafalla H, Akhtar S, et al. PEGylated green halloysite/spinel ferrite nanocomposites for pH sensitive delivery of dexamethasone: a potential pulmonary drug delivery treatment option for COVID-19. Appl Clay Sci 2022;216:106333.
[28] Xiong J, Xie R, Wang Y, Wang C, Ai Y, Zheng W, et al. Nitrite-responsive hydrogel: smart drug release depending on the severity of the nitric oxide-related disease. ACS Appl Mater Interfaces 2020;12(46):51185–97.
[29] Xu L, Zhang X, Chu Z, Wang H, Li Y, Shen X, et al. Temperature-responsive multilayer films based on block copolymer-coated silica nanoparticles for long-term release of. ACS Appl Nano Mater 2021;4(12):14014–25.
[30] Nabil A, Yoshihara E, Hironaka K, Hassan AA, Shiha G, Ebara M. Temperature responsive smart polymer for enabling affinity enrichment of current coronavirus (SARS-CoV-2) to improve its diagnostic sensitivity. Comput Struct Biotechnol J 2021;19:3609–17.
[31] Fonseca B, Fonseca C, Barros M, White M, Abhyankar V, Borkholder DA, et al. Ultrasound-based control of micro-bubbles for exosome delivery in treating COVID-19 lung damage. In: 2021 IEEE International Conference on Communications Workshops (ICC Workshops); Montreal, QC, Canada; 2021. p. 1–6.
[32] Martins ES, Espindola A, Britos TN, Chagas C, Barbosa E,

Castro CE, et al. Potential use of DMSA-containing iron oxide nanoparticles as magnetic vehicles against the COVID-19 disease. ChemistrySelect 2021;6(31):7931–5.
[33] Ebrahimi S, Shamloo A, Alishiri M, Mofrad YM, Akherati F. Targeted pulmonary drug delivery in coronavirus disease (COVID-19) therapy: a patient-specific in silico study based on magnetic nanoparticles-coated microcarriers adhesion. Int J Pharm 2021;609:121133.
[34] Varshosaz J, Javanmard SH, Soghrati S, Behdadfar B. Magnetic chondroitin targeted nanoparticles for dual targeting of montelukast in prevention of in-stent restenosis. RSC Adv 2016;6(15):12337–47.
[35] D'Autréaux B, Toledano MB. ROS as signalling molecules: mechanisms that generate specificity in ROS homeostasis. Nat Rev Mol Cell Biol 2007;8(10):813–24.
[36] Hayyan M, Hashim MA, AlNashef IM. Superoxide ion: generation and chemical implications. Chem Rev 2016;116(5):3029–85.
[37] Salman KA, Ashraf S. Reactive oxygen species: a link between chronic inflammation and cancer. Asia-Pacific J Mol Biol Biotechnol 2013;21:41–9.
[38] Guo X, Cheng Y, Zhao X, Luo Y, Chen J, Yuan W. Advances in redox-responsive drug delivery systems of tumor microenvironment. J Nanobiotechnology 2018;16(1):74.
[39] Brieger K, Schiavone S, Miller FJ, Krause KH. Reactive oxygen species: from health to disease. Swiss Med Wkly 2012;142:w13659.
[40] Kalyanaraman B. Reactive oxygen species, proinflammatory and immunosuppressive mediators induced in COVID-19: overlapping biology with cancer. RSC Chem Biol 2021;2(5):1402–14.
[41] Amini MA, Talebi SS, Karimi J. Reactive oxygen species modulator 1 (ROMO1), a new potential target for cancer diagnosis and treatment. Chonnam Med J 2019;55(3):136–43.
[42] Chouaki Benmansour N, Carvelli J, Vivier E. Complement cascade in severe forms of COVID-19: recent advances in therapy. Eur J Immunol 2021;51(7):1652–9.
[43] Chen L, Hong W, Ren W, Xu T, Qian Z, He Z. Recent progress in targeted delivery vectors based on biomimetic nanoparticles. Signal Transduct Target Ther 2021;6(1):1–25.
[44] Mathi K, Rosenberg-Hasson Y, Maecker H, Carlo DJ, Moss RB. Brief report: tempol, a novel antioxidant, inhibits both activated T cell and antigen presenting cell derived cytokines in-vitro from COVID-19 patients. Clin Immunol 2021;231:108828.
[45] Ren H, Wu Y, Ma N, Xu H, Zhang X. Side-chain selenium-containing amphiphilic block copolymers: redox-controlled self-assembly and disassembly. Soft Matter 2012;8(5):1460–6.
[46] Xu H, Cao W, Zhang X. Selenium-containing polymers: promising biomaterials for controlled release and enzyme mimics. Acc Chem Res 2013;46(7):1647–58.
[47] Jeong D, Bae BC, Park SJ, Na K. Reactive oxygen species responsive drug releasing nanoparticle based on chondroitin sulfate–anthocyanin nanocomplex for efficient tumor therapy. J Control Release 2016;222:78–85.
[48] Leong J, Chin W, Ke X, Gao S, Kong H, Hedrick JL, et al. Disease-directed design of biodegradable polymers: reactive oxygen species and pH-responsive micellar nanoparticles for anticancer drug delivery. Nanomedicine 2018;14(8):2666–77.
[49] Scott EA, Stano A, Gillard M, Maio-Liu AC, Swartz MA, Hubbell JA. Dendritic cell activation and T cell priming with adjuvant-and antigen-loaded oxidation-sensitive polymersomes. Biomaterials 2012;33(26):6211–19.
[50] Dollinger BR, Gupta MK, Martin JR, Duvall CL. Reactive oxygen species shielding hydrogel for the delivery of adherent and nonadherent therapeutic cell types. Tissue Eng Part A 2017;23(19–20):1120–31.
[51] Poole KM, Nelson CE, Joshi RV, Martin JR, Gupta MK, Haws SC, et al. ROS-responsive microspheres for on demand antioxidant therapy in a model of diabetic peripheral arterial disease. Biomaterials 2015;41:166–75.
[52] Saravanakumar G, Lee J, Kim J, Kim WJ. Visible light-induced singlet oxygen-mediated intracellular disassembly of polymeric micelles co-loaded with a photosensitizer and an anticancer drug for enhanced photodynamic therapy. Chem Commun 2015;51(49):9995–8.
[53] Yao Y, Ding J, Wang Z, Zhang H, Xie J, Wang Y, et al. ROS-responsive polyurethane fibrous patches loaded with methylprednisolone (MP) for restoring structures and functions of infarcted myocardium *in vivo*. Biomaterials 2020;232:119726.
[54] Shim MS, Xia Y. A reactive oxygen species (ROS)-responsive polymer for safe, efficient, and targeted gene delivery in cancer cells. Angew Chem Int Ed Engl 2013;125(27):7064–7.
[55] Regmi S, Pathak S, Nepal MR, Shrestha P, Park J, Kim JO, et al. Inflammation-triggered local drug release ameliorates colitis by inhibiting dendritic cell migration and Th1/Th17 differentiation. J Control Release 2019;316:138–49.
[56] Li J, Sun C, Tao W, Cao Z, Qian H, Yang X, et al. Photoinduced PEG deshielding from ROS-sensitive linkage-bridged block copolymer-based nanocarriers for on-demand drug delivery. Biomaterials 2018;170:147–55.
[57] Cao W, Gu Y, Li T, Xu H. Ultra-sensitive ROS-responsive tellurium-containing polymers. Chem Commun 2015;51(32):7069–71.
[58] Zhang Q, Zhang F, Chen Y, Dou Y, Tao H, Zhang D, et al. Structure–property correlations of reactive oxygen species-responsive and hydrogen peroxide-eliminating materials with anti-oxidant and anti-inflammatory activities. Chem Mater 2017;29(19):8221–38.
[59] Lin L, Gong H, Li R, Huang J, Cai M, Lan T, et al. Nanodrug with ROS and pH dual-sensitivity ameliorates liver fibrosis via multicellular regulation. Adv Sci 2020;7(7):1903138.
[60] Zhu D, Yan H, Liu X, Xiang J, Zhou Z, Tang J, et al. Intracellularly disintegratable polysulfoniums for efficient gene delivery. Adv Funct Mater 2017;27(16):1606826.
[61] Broaders KE, Grandhe S, Fréchet JM. A biocompatible oxidation-triggered carrier polymer with potential in therapeutics. J Am Chem Soc 2011;133(4):756–8.
[62] Ko E, Jeong D, Kim J, Park S, Khang G, Lee D. Antioxidant polymeric prodrug microparticles as a therapeutic system for acute liver failure. Biomaterials 2014;35(12):3895–902.
[63] Cho B-R, Ryu DR, Lee K-S, Lee D-K, Bae S, Kang DG, et al. Hydroxybenzyl alcohol-containing biodegradable nanoparticle improves functional blood flow through angiogenesis in a mouse model of hindlimb ischemia. Biomaterials 2015;53:679–87.
[64] Yu SS, Koblin RL, Zachman AL, Perrien DS, Hofmeister LH, Giorgio TD, et al. Physiologically relevant oxidative degradation of oligo (proline) cross-linked polymeric scaffolds. Biomacromolecules 2011;12(12):4357–66.
[65] Rodriguez AR, Kramer JR, Deming TJ. Enzyme-triggered cargo release from methionine sulfoxide containing copolypeptide vesicles. Biomacromolecules 2013;14(10):3610–14.
[66] Xu F, Li H, Luo YL, Tang W. Redox-responsive self-assembly micelles from poly (N-acryloylmorpholine-block-2-acryloyloxyethyl ferrocenecarboxylate) amphiphilic block copolymers as drug release carriers. ACS Appl Mater Interfaces 2017;9(6):5181–92.
[67] Park W, Bae BC, Na K. A highly tumor-specific light-triggerable drug carrier responds to hypoxic tumor

conditions for effective tumor treatment. Biomaterials 2016;77:227–34.
[68] Rao V, Han HS, Lee H, Jeon S, Jung DW, Lee J, et al. ROS-responsive mesoporous silica nanoparticles for MR imaging-guided photodynamically maneuvered chemotherapy. Nanoscale 2018;10(20):9616–27.
[69] Kim H, Kim Y, Kim IH, Kim K, Choi Y. ROS-responsive activatable photosensitizing agent for imaging and photodynamic therapy of activated macrophages. Theranostics 2014;4(1):1–11.
[70] Teo JY, Seo Y, Ko E, Leong J, Hong YT, Yang YY, et al. Surface tethering of stem cells with H2O2-responsive anti-oxidizing colloidal particles for protection against oxidation-induced death. Biomaterials 2019;201:1–15.
[71] Chen Q, Feng L, Liu J, Zhu W, Dong Z, Wu Y, et al. Intelligent albumin–$MnO_2$ nanoparticles as pH-/$H_2O_2$-responsive dissociable nanocarriers to modulate tumor hypoxia for effective combination therapy. Adv Mater 2016;28(33):7129–36.
[72] Wu H, Li F, Wang S, Lu J, Li J, Du Y, et al. Ceria nanocrystals decorated mesoporous silica nanoparticle based ROS-scavenging tissue adhesive for highly efficient regenerative wound healing. Biomaterials 2018;151:66–77.
[73] Shen Y, Cao B, Snyder NR, Woeppel KM, Eles JR, Cui XT. ROS responsive resveratrol delivery from LDLR peptide conjugated PLA-coated mesoporous silica nanoparticles across the blood–brain barrier. J Nanobiotechnology 2018;16(1):1–17.
[74] Li H, He J, Zhang M, Liu J, Ni P. Glucose-sensitive polyphosphoester diblock copolymer for an insulin delivery system. ACS Biomater Sci Eng 2020;6(3):1553–64.
[75] Zhong Y, Song B, He D, Xia Z, Wang P, Wu J, et al. Galactose-based polymer-containing phenylboronic acid as carriers for insulin delivery. Nanotechnology 2020;31(39):395601.
[76] Wang J, Yu J, Zhang Y, Zhang X, Kahkoska AR, Chen G, et al. Charge-switchable polymeric complex for glucose-responsive insulin delivery in mice and pigs. Sci Adv 2019;5(7):eaaw4357.
[77] Ardestani A, Azizi Z. Targeting glucose metabolism for treatment of COVID-19. Signal Transduct Target Ther 2021;6(1):112.
[78] Zoulikha M, Huang F, Wu Z, He W. COVID-19 inflammation and implications in drug delivery. J Control Release 2022;346:260–74.
[79] Dou Y, Li C, Li L, Guo J, Zhang J. Bioresponsive drug delivery systems for the treatment of inflammatory diseases. J Control Release 2020;327:641–66.
[80] Sreedhar A, Zhao Y. Dysregulated metabolic enzymes and metabolic reprogramming in cancer cells. Biomed Rep 2018;8(1):3–10.
[81] Fan C, Shi J, Zhuang Y, Zhang L, Huang L, Yang W, et al. Myocardial-infarction-responsive smart hydrogels targeting matrix metalloproteinase for on-demand growth factor delivery. Adv Mater 2019;31(40):1902900.
[82] Yao Q, Dai Z, Hoon Choi J, Kim D, Zhu L. Building stable MMP2-responsive multifunctional polymeric micelles by an all-in-one polymer–lipid conjugate for tumor-targeted intracellular drug delivery. ACS Appl Mater Interfaces 2017;9(38):32520–33.
[83] Szilágyi BÁ, Némethy Á, Magyar A, Szabó I, Bősze S, Gyarmati B, et al. Amino acid based polymer hydrogel with enzymatically degradable cross-links. React Funct Polym 2018;133:21–8.
[84] Mejías JC, Forrest OA, Margaroli C, Rubio DAF, Viera L, Li J, et al. Neutrophil-targeted, protease-activated pulmonary drug delivery blocks airway and systemic inflammation. JCI insight 2019;4(23):e131468.
[85] Ding H, Zhang F, Zhao C, Lv Y, Ma G, Wei W, et al. Beyond a carrier: graphene quantum dots as a probe for programmatically monitoring anti-cancer drug delivery, release, and response. ACS Appl Mater Interfaces 2017;9(33):27396–401.
[86] Chen Y, Guo M, Qu D, Liu Y, Guo J, Chen Y. Furin-responsive triterpenine-based liposomal complex enhances anticervical cancer therapy through size modulation. Drug Deliv 2020;27(1):1608–24.
[87] Jiang T, Sun W, Zhu Q, Burns NA, Khan SA, Mo R, et al. Furin-mediated sequential delivery of anticancer cytokine and small-molecule drug shuttled by graphene. Adv Mater 2015;27(6):1021–8.
[88] Li K, Sato H, Kim CW, Nakamura Y, Zhao GX, Funamoto D, et al. Tumor accumulation of protein kinase-responsive gene carrier/DNA polyplex stabilized by alkanethiol for intravenous injection. J Biomater Sci Polym Ed 2015;26(11):657–68.
[89] Kang JH, Asai D, Kim JH, Mori T, Toita R, Tomiyama T, et al. Design of polymeric carriers for cancer-specific gene targeting: utilization of abnormal protein kinase $C\alpha$ activation in cancer cells. J Am Chem Soc 2008;130(45):14906–7.
[90] Zhao N, Wu B, Hu X, Xing D. NIR-triggered high-efficient photodynamic and chemo-cascade therapy using caspase-3 responsive functionalized upconversion nanoparticles. Biomaterials 2017;141:40–9.
[91] Gu Z, Yan M, Hu B, Joo KI, Biswas A, Huang Y, et al. Protein nanocapsule weaved with enzymatically degradable polymeric network. Nano Lett 2009;9(12):4533–8.
[92] Guo J, Li D, Tao H, Li G, Liu R, Dou Y, et al. Cyclodextrin-derived intrinsically bioactive nanoparticles for treatment of acute and chronic inflammatory diseases. Adv Mater 2019;31(46):1904607.
[93] Zhuo S, Zhang F, Yu J, Zhang X, Yang G, Liu X. pH-sensitive biomaterials for drug delivery. Molecules 2020;25(23):5649.
[94] Patra JK, Das G, Fraceto LF, Campos EVR, MdP Rodriguez-Torres, Acosta-Torres LS, et al. Nano based drug delivery systems: recent developments and future prospects. J Nanobiotechnology 2018;16(1):1–33.
[95] Sun Y, Davis E. Nanoplatforms for targeted stimuli-responsive drug delivery: a review of platform materials and stimuli-responsive release and targeting mechanisms. Nanomater 2021;11(3):746.
[96] Boedtkjer E, Pedersen SF. The acidic tumor microenvironment as a driver of cancer. Annu Rev Physiol 2020;82:103–26.
[97] Duan Z, Zhao Q, Wang S, Huang Q, Yuan Z, Zhang Y, et al. Halloysite nanotubes: natural, environmental-friendly and low-cost nanomaterials for high-performance humidity sensor. Sens Actuators B Chem 2020;317:128204.
[98] Sharpe LA, Vela Ramirez JE, Haddadin OM, Ross KA, Narasimhan B, Peppas NA. pH-responsive microencapsulation systems for the oral delivery of polyanhydride nanoparticles. Biomacromolecules 2018;19(3):793–802.
[99] Rayamajhi S, Marchitto J, Nguyen TDT, Marasini R, Celia C, Aryal S. pH-responsive cationic liposome for endosomal escape mediated drug delivery. Colloids Surf B Biointerfaces 2020;188:110804.
[100] Son I, Lee Y, Baek J, Park M, Han D, Min SK, et al. pH-Responsive amphiphilic polyether micelles with superior stability for smart drug delivery. Biomacromolecules 2021;22(5):2043–56.
[101] Afzal S, Samiullah K, Ranjha NM, Jalil A, Amina R, Haider MS, et al. The structural, crystallinity, and thermal properties of pH-responsive interpenetrating gelatin/sodium

alginate-based polymeric composites for the controlled delivery of cetirizine HCl. Turk J Pharm Sci 2018;15(1):63.
[102] Coban O, Aytac Z, Yildiz ZI, Uyar T. Colon targeted delivery of niclosamide from β-cyclodextrin inclusion complex incorporated electrospun Eudragit® L100 nanofibers. Colloids Surf B Biointerfaces 2021;197:111391.
[103] Mu M, Liang X, Chuan D, Zhao S, Yu W, Fan R, et al. Chitosan coated pH-responsive metal-polyphenol delivery platform for melanoma chemotherapy. Carbohydr Polym 2021;264:118000.
[104] Sathiyaseelan A, Saravanakumar K, Mariadoss AVA, Wang MH. pH-controlled nucleolin targeted release of dual drug from chitosan-gold based aptamer functionalized nano drug delivery system for improved glioblastoma treatment. Carbohydr Polym 2021;262:117907.
[105] Luo J, Li X, Dong S, Zhu P, Liu W, Zhang S, et al. Layer-by-layer coated hybrid nanoparticles with pH-sensitivity for drug delivery to treat acute lung infection. Drug Deliv 2021;28(1):2460–8.
[106] Gisbert-Garzaran M, Berkmann JC, Giasafaki D, Lozano D, Spyrou K, Manzano M, et al. Engineered pH-responsive mesoporous carbon nanoparticles for drug delivery. ACS Appl Mater Interfaces 2020;12(13):14946–57.
[107] Mutalik S, Suthar NA, Managuli RS, Shetty PK, Avadhani K, Kalthur G, et al. Development and performance evaluation of novel nanoparticles of a grafted copolymer loaded with curcumin. Int J Biol Macromol 2016;86:709–20.
[108] Yeo J, Lee YM, Lee J, Park D, Kim K, Kim J, et al. Nitric oxide-scavenging nanogel for treating rheumatoid arthritis. Nano Lett 2019;19(10):6716–24.
[109] Ali Zolfigol M, Shirini F, Choghamarani AG. Mohammadpoor-Baltork I. Silica Chloride/$NaNO_2$ as a novel heterogeneous system for the oxidation of 1, 4-dihydropyridines under mild conditions via *in situ* generation of NOCl. Phosphorus Sulfur Silicon Relat Elem 2003;178(8):1709–15.
[110] Alamdari DH, Moghaddam AB, Amini S, Keramati MR, Zarmehri AM, Alamdari AH, et al. Application of methylene blue-vitamin C–N-acetyl cysteine for treatment of critically ill COVID-19 patients, report of a phase-I clinical trial. Eur J Pharmacol 2020;885:173494.
[111] Karimi M, Sahandi Zangabad P, Ghasemi A, Amiri M, Bahrami M, Malekzad H, et al. Temperature-responsive smart nanocarriers for delivery of therapeutic agents: applications and recent advances. ACS Appl Mater Interfaces 2016;8(33):21107–33.
[112] Hegyi G, Szigeti GP, Szász A. Hyperthermia *versus* oncothermia: cellular effects in complementary cancer therapy. Evid Based Complementary Altern Med 2013;2013:672873.
[113] Eleftheriou K, Kaminari A, Panagiotaki KN, Sideratou Z, Zachariadis M, Anastassopoulou J, et al. A combination drug delivery system employing thermosensitive liposomes for enhanced cell penetration and improved *in vitro* efficacy. Int J Pharm 2020;574:118912.
[114] Ye H, Chu X, Cao Z, Hu X, Wang Z, Li M, et al. A novel targeted therapy system for cervical cancer: co-delivery system of antisense LncRNA of MDC1 and oxaliplatin magnetic thermosensitive cationic liposome drug carrier. Int J Nanomedicine 2021;16:1051.
[115] Liu C, Guo X, Ruan C, Hu H, Jiang BP, Liang H, et al. An injectable thermosensitive photothermal-network hydrogel for near-infrared-triggered drug delivery and synergistic photothermal-chemotherapy. Acta Biomater 2019;96:281–94.
[116] Rejinold NS, Sreerekha P, Chennazhi K, Nair S, Biocompatible Jayakumar R. biodegradable and thermo-sensitive chitosan-g-poly (N-isopropylacrylamide) nanocarrier for curcumin drug delivery. Int J Biol Macromol 2011;49(2):161–72.
[117] Chan PS, Xian JW, Li Q, Chan CW, Leung SS, To KK. Biodegradable thermosensitive PLGA-PEG-PLGA polymer for non-irritating and sustained ophthalmic drug delivery. AAPS J 2019;21(4):1–13.
[118] Kim C, Guo Y, Velalopoulou A, Leisen J, Motamarry A, Ramajayam K, et al. Closed-loop trans-skull ultrasound hyperthermia leads to improved drug delivery from thermosensitive drugs and promotes changes in vascular transport dynamics in brain tumors. Theranostics 2021;11(15):7276.
[119] Wei Y, Li C, Zhu Q, Zhang X, Guan J, Mao S. Comparison of thermosensitive *in situ* gels and drug-resin complex for ocular drug delivery: *in vitro* drug release and *in vivo* tissue distribution. Int J Pharm 2020;578:119184.
[120] Zou H, Sun H, Wang L, Zhao L, Li J, Dong Z, et al. Construction of a smart temperature-responsive GPx mimic based on the self-assembly of supra-amphiphiles. Soft Matter 2016;12(4):1192–9.
[121] Petrini M, Lokerse WJ, Mach A, Hossann M, Merkel OM, Lindner LH. Effects of surface charge, PEGylation and functionalization with dipalmitoylphosphatidyldiglycerol on liposome–cell interactions and local drug delivery to solid tumors via thermosensitive liposomes. Int J Nanomedicine 2021;16:4045.
[122] Du C, Li S, Li Y, Galons H, Guo N, Teng Y, et al. F7 and topotecan co-loaded thermosensitive liposome as a nano-drug delivery system for tumor hyperthermia. Drug Deliv 2020;27(1):836–47.
[123] Ohya S, Nakayama Y, Matsuda T. Thermoresponsive artificial extracellular matrix for tissue engineering: hyaluronic acid bioconjugated with poly (N-isopropylacrylamide) grafts. Biomacromolecules 2001;2(3):856–63.
[124] Park KM, Bae JW, Joung YK, Shin JW, Park KD. Nanoaggregate of thermosensitive chitosan-Pluronic for sustained release of hydrophobic drug. Colloids Surf B Biointerfaces 2008;63(1):1–6.
[125] Zeighamian V, Darabi M, Akbarzadeh A, Rahmati-Yamchi M, Zarghami N, Badrzadeh F, et al. PNIPAAm-MAA nanoparticles as delivery vehicles for curcumin against MCF-7 breast cancer cells. Artif Cells Nanomed Biotechnol 2016;44(2):735–42.
[126] Huang Q, Du C, Hua Y, Zhang J, Peng R, Yao X. Synthesis and characterization of loaded Nano/zinc oxide composite hydrogels intended for anti-mold coatings on bamboo. Bioresources 2019;14(3):7134–47.
[127] Saeednia L, Yao L, Cluff K, Asmatulu R. Sustained releasing of methotrexate from injectable and thermosensitive chitosan–carbon nanotube hybrid hydrogels effectively controls tumor cell growth. ACS Omega 2019;4(2):4040–8.
[128] Rezazadeh M, Akbari V, Varshosaz J, Karbasizadeh P, Minaiyan M. Sustained-release of erythropoietin using a novel injectable thermosensitive hydrogel: *in vitro* studies, biological activity, and efficacy in rats. Pharm Dev Technol 2021;26(4):412–21.
[129] Singh A, Vaishagya K, Verma RK, Shukla R. Temperature/pH-triggered PNIPAM-based smart nanogel system loaded with anastrozole delivery for application in cancer chemotherapy. AAPS PharmSciTech 2019;20(5):213.
[130] Metawea OR, Abdelmoneem MA, Haiba NS, Khalil HH, Teleb M, Elzoghby AO, et al. A novel 'smart'PNIPAM-based copolymer for breast cancer targeted therapy: synthesis, and characterization of dual pH/temperature-responsive lactoferrin-targeted PNIPAM-co-AA. Colloids Surf B Biointerfaces 2021;202:111694.
[131] Zheng L, Huang X, Lin X, Lin W, Yang F, Chen T. Thermosensitive hydrogels for sustained-release

of sorafenib and selenium nanoparticles for localized synergistic chemoradiotherapy. Biomaterials 2019;216:119220.
[132] Don TM, Lu KY, Lin LJ, Hsu CH, Wu JY, Mi FL. Temperature/pH/enzyme triple-responsive cationic protein/PAA-b-PNIPAAm nanogels for controlled anticancer drug and photosensitizer delivery against multidrug resistant breast cancer cells. Mol Pharm 2017;14(12):4648–60.
[133] Huebsch N, Kearney CJ, Zhao X, Kim J, Cezar CA, Suo Z, et al. Ultrasound-triggered disruption and self-healing of reversibly cross-linked hydrogels for drug delivery and enhanced chemotherapy. Proc Natl Acad Sci USA 2014;111(27):9762–7.
[134] Izadifar Z, Izadifar Z, Chapman D, Babyn P. An introduction to high intensity focused ultrasound: systematic review on principles, devices, and clinical applications. J Clin Med 2020;9(2):460.
[135] Mulvana H, Browning RJ, Luan Y, De Jong N, Tang MX, Eckersley RJ, et al. Characterization of contrast agent microbubbles for ultrasound imaging and therapy research. IEEE Trans Ultrason Ferroelectr Freq Control 2016;64(1):232–51.
[136] Sengupta V, Sengupta S, Lazo A, Woods P, Nolan A, Bremer N. Exosomes derived from bone marrow mesenchymal stem cells as treatment for severe COVID-19. Stem Cells Dev 2020;29(12):747–54.
[137] Sanwal R, Joshi K, Ditmans M, Tsai SS, Lee WL. Ultrasound and microbubbles for targeted drug delivery to the lung endothelium in ARDS: cellular mechanisms and therapeutic opportunities. Biomedicines 2021;9(7):803.
[138] Min KH, Min HS, Lee HJ, Park DJ, Yhee JY, Kim K, et al. pH-controlled gas-generating mineralized nanoparticles: a theranostic agent for ultrasound imaging and therapy of cancers. ACS Nano 2015;9(1):134–45.
[139] Bhandari P, Novikova G, Goergen CJ, Irudayaraj J. Ultrasound beam steering of oxygen nanobubbles for enhanced bladder cancer therapy. Sci Rep 2018;8(1):1–10.
[140] Tayier B, Deng Z, Wang Y, Wang W, Mu Y, Yan F. Biosynthetic nanobubbles for targeted gene delivery by focused ultrasound. Nanoscale 2019;11(31):14757–68.
[141] Meng M, Gao J, Wu C, Zhou X, Zang X, Lin X, et al. Doxorubicin nanobubble for combining ultrasonography and targeted chemotherapy of rabbit with VX2 liver tumor. Tumor Biol 2016;37(7):8673–80.
[142] Jiang Q, Hao S, Xiao X, Yao J, Ou B, Zhao Z, et al. Production and characterization of a novel long-acting Herceptin-targeted nanobubble contrast agent specific for Her-2-positive breast cancers. Breast Cancer 2016;23(3):445–55.
[143] Zhang B, Chen M, Zhang Y, Chen W, Zhang L, Chen L. An ultrasonic nanobubble-mediated PNP/fludarabine suicide gene system: a new approach for the treatment of hepatocellular carcinoma. PLoS One 2018;13(5):e0196686.
[144] Shen S, Li Y, Xiao Y, Zhao Z, Zhang C, Wang J, et al. Folate-conjugated nanobubbles selectively target and kill cancer cells via ultrasound-triggered intracellular explosion. Biomaterials 2018;181:293–306.
[145] Tian Y, Liu Z, Zhang L, Zhang J, Han X, Wang Q, et al. Apatinib-loaded lipid nanobubbles combined with ultrasound-targeted nanobubble destruction for synergistic treatment of HepG2 cells *in vitro*. Onco Targets Ther 2018;11:4785.
[146] Shang M, Wang K, Guo L, Duan S, Lu Z, Li J. Development of novel ST68/PLA-PEG stabilized ultrasound nanobubbles for potential tumor imaging and theranostic. Ultrasonics 2019;99:105947.
[147] Song W, Luo Y, Zhao Y, Liu X, Zhao J, Luo J, et al. Magnetic nanobubbles with potential for targeted drug delivery and trimodal imaging in breast cancer: an *in vitro* study. Nanomedicine 2017;12(9):991–1009.
[148] Li Y, Wan J, Zhang Z, Guo J, Wang C. Targeted soft biodegradable glycine/PEG/RGD-modified poly (methacrylic acid) nanobubbles as intelligent theranostic vehicles for drug delivery. ACS Appl Mater Interfaces 2017;9(41):35604–12.
[149] Wang Y, Sui G, Teng D, Wang Q, Qu J, Zhu L, et al. Low intensity focused ultrasound (LIFU) triggered drug release from cetuximab-conjugated phase-changeable nanoparticles for precision theranostics against anaplastic thyroid carcinoma. Biomater Sci 2019;7(1):196–210.
[150] Tang W, Yang Z, Wang S, Wang Z, Song J, Yu G, et al. Organic semiconducting photoacoustic nanodroplets for laser-activatable ultrasound imaging and combinational cancer therapy. ACS Nano 2018;12(3):2610–22.
[151] Ho YJ, Chiang YJ, Kang ST, Fan CH, Yeh CK. Camptothecin-loaded fusogenic nanodroplets as ultrasound theranostic agent in stem cell-mediated drug-delivery system. J Control Release 2018;278:100–9.
[152] Başpınar Y, Erel-Akbaba G, Kotmakçı M, Akbaba H. Development and characterization of nanobubbles containing paclitaxel and survivin inhibitor YM155 against lung cancer. Int J Pharm 2019;566:149–56.
[153] Yu M, Xu X, Cai Y, Zou L, Shuai X. Perfluorohexane-cored nanodroplets for stimulations-responsive ultrasonography and $O_2$-potentiated photodynamic therapy. Biomaterials 2018;175:61–71.
[154] Meng D, Guo L, Shi D, Sun X, Shang M, Zhou X, et al. Charge-conversion and ultrasound-responsive O-carboxymethyl chitosan nanodroplets for controlled drug delivery. Nanomedicine (Lond) 2019;14(19):2549–65.
[155] Mannaris C, Yang C, Carugo D, Owen J, Lee JY, Nwokeoha S, et al. Acoustically responsive polydopamine nanodroplets: a novel theranostic agent. Ultrason Sonochem 2020;60:104782.
[156] Dong X, Lu X, Kingston K, Brewer E, Juliar BA, Kripfgans OD, et al. Controlled delivery of basic fibroblast growth factor (bFGF) using acoustic droplet vaporization stimulates endothelial network formation. Acta Biomater 2019;97:409–19.
[157] Soto F, Jeerapan I, Silva-López C, Lopez-Ramirez MA, Chai I, Xiaolong L, et al. Noninvasive transdermal delivery system of lidocaine using an acoustic droplet-vaporization based wearable patch. Small 2018;14(49):1803266.
[158] Issa B, Obaidat IM, Albiss BA, Haik Y. Magnetic nanoparticles: surface effects and properties related to biomedicine applications. Int J Mol Sci 2013;14(11):21266–305.
[159] Askari E, Seyfoori A, Amereh M, Gharaie SS, Ghazali HS, Ghazali ZS, et al. Stimuli-responsive hydrogels for local post-surgical drug delivery. Gels 2020;6(2):14.
[160] Abo-Zeid Y, Ismail NS, McLean GR, Hamdy NM. A molecular docking study repurposes FDA approved iron oxide nanoparticles to treat and control COVID-19 infection. Eur J Pharm Sci 2020;153:105465.
[161] Das SS, Bharadwaj P, Bilal M, Barani M, Rahdar A, Taboada P, et al. Stimuli-responsive polymeric nanocarriers for drug delivery, imaging, and theragnosis. Polymers 2020;12(6):1397.
[162] Wang X, Xuan Z, Zhu X, Sun H, Li J, Xie Z. Near-infrared photoresponsive drug delivery nanosystems for cancer photo-chemotherapy. J Nanobiotechnology 2020;18:1–19.
[163] Zhao H, Sterner ES, Coughlin EB, Theato P. o-Nitrobenzyl alcohol derivatives: opportunities in polymer and materials science. Macromolecules 2012;45(4):1723–36.
[164] Scholle K, Lamrini S, Koopmann P, Fuhrberg P. 2 µm Laser sources and their possible applications. In: Pal B, editor. Frontiers in guided wave optics and optoelectronics. London: IntechOpen; 2010. p. 471.

[165] Karimi M, Sahandi Zangabad P, Baghaee-Ravari S, Ghazadeh M, Mirshekari H, Hamblin MR. Smart nanostructures for cargo delivery: uncaging and activating by light. J Am Chem Soc 2017;139(13):4584–610.
[166] Miranda D, Lovell JF. Mechanisms of light-induced liposome permeabilization. Bioeng Transl Med 2016;1(3):267–76.
[167] Olejniczak J, Carling CJ, Almutairi A. Photocontrolled release using one-photon absorption of visible or NIR light. J Control Release 2015;219:18–30.
[168] Seo Y, Park K, Hong Y, Lee ES, Kim SS, Jung YT, et al. Reactive-oxygen-species-mediated mechanism for photoinduced antibacterial and antiviral activities of $Ag_3PO_4$. J Anal Sci Technol 2020;11(1):1–6.
[169] Pourhajibagher M, Azimi M, Haddadi-Asl V, Ahmadi H, Gholamzad M, Ghorbanpour S, et al. Robust antimicrobial photodynamic therapy with curcumin-poly (lactic-co-glycolic acid) nanoparticles against COVID-19: a preliminary *in vitro* study in vero cell line as a model. Photodiagnosis Photodyn Ther 2021;34:102286.
[170] Svyatchenko VA, Nikonov SD, Mayorov AP, Gelfond ML, Loktev VB. Antiviral photodynamic therapy: inactivation and inhibition of SARS-CoV-2 *in vitro* using methylene blue and Radachlorin. Photodiagnosis Photodyn Ther 2021;33:102112.
[171] Sachet P, Rocha BA, Lima FS, da Silva Pedrosa M, Guollo A, de Melo Filho MR, et al. Management of orofacial lesions with antimicrobial photodynamic therapy and photobiomodulation protocols in patients with COVID-19: a multicenter case series. Photodiagnosis Photodyn Ther 2022;38:102743.
[172] Schikora D, Hepburn J, Plavin SR. Reduction of the viral load by non-invasive photodynamic therapy in early stages of COVID-19 infection. Am J Virol Dis 2020;2(1):01–5.
[173] Cagno V, Medaglia C, Cerny A, Cerny T, Zwygart ACA, Cerny E, et al. Methylene blue has a potent antiviral activity against SARS-CoV-2 and H1N1 influenza virus in the absence of UV-activation *in vitro*. Sci Rep 2021;11(1):1–8.
[174] Gendrot M, Andreani J, Duflot I, Boxberger M, Le Bideau M, Mosnier J, et al. Methylene blue inhibits replication of SARS-CoV-2 *in vitro*. Int J Antimicrob Agents 2020;56(6):106202.
[175] Li JY, Qiu L, Xu XF, Pan CY, Hong CY, Zhang WJ. Photo-responsive camptothecin-based polymeric prodrug coated silver nanoparticles for drug release behaviour tracking via the nanomaterial surface energy transfer (NSET) effect. J Mater Chem B 2018;6(11):1678–87.
[176] Zhang Y, Lu G, Yu Y, Zhang H, Gao J, Sun Z, et al. NIR-responsive copolymer upconversion nanocomposites for triggered drug release *in vitro* and *in vivo*. ACS Appl Bio Mater 2018;2(1):495–503.
[177] Liu Z, Shi J, Wang Y, Gan Y, Wan P. Facile preparation of pyrenemethyl ester-based nanovalve on mesoporous silica coated upconversion nanoparticle for NIR light-triggered drug release with potential monitoring capability. Colloids Surf A Physicochem Eng Asp 2019;568:436–44.
[178] Long K, Yang Y, Lv W, Jiang K, Li Y, Lo ACY, et al. Green light-triggered intraocular drug release for intravenous chemotherapy of retinoblastoma. Adv Sci 2021;8(20):2101754.
[179] Babin J, Pelletier M, Lepage M, Allard JF, Morris D, Zhao Y. A new two-photon-sensitive block copolymer nanocarrier. Angew Chem Int Ed Engl 2009;48(18):3329–32.
[180] Kumar S, Allard JF, Morris D, Dory YL, Lepage M, Zhao Y. Near-infrared light sensitive polypeptide block copolymer micelles for drug delivery. J Mater Chem 2012;22(15):7252–7.
[181] He S, Krippes K, Ritz S, Chen Z, Best A, Butt HJ, et al. Ultralow-intensity near-infrared light induces drug delivery by upconverting nanoparticles. Chem Commun 2015;51(2):431–4.
[182] Englert C, Nischang I, Bader C, Borchers P, Alex J, Pröhl M, et al. Photocontrolled release of chemicals from nano-and microparticle containers. Angew Chem Int Ed Engl 2018;57(9):2479–82.
[183] Croissant JG, Qi C, Mongin O, Hugues V, Blanchard-Desce M, Raehm L, et al. Disulfide-gated mesoporous silica nanoparticles designed for two-photon-triggered drug release and imaging. J Mater Chem B 2015;3(31):6456–61.
[184] Yavlovich A, Viard M, Gupta K, Sine J, Vu M, Blumenthal R, et al. Low-visibility light-intensity laser-triggered release of entrapped calcein from 1, 2-bis (tricosa-10, 12-diynoyl)-*sn*-glycero-3-phosphocholine liposomes is mediated through a type I photoactivation pathway. Int J Nanomedicine 2013;8:2575.
[185] Hammond GS, Stout CA, Lamola AA. Mechanisms of photochemical reactions in solution. XXV. The photodimerization of coumarin. J Am Chem Soc 1964;86(15):3103–6.
[186] Li J, Li X, Liu H, Ren T, Huang L, Deng Z, et al. GSH and light dual stimuli-responsive supramolecular polymer drug carriers for cancer therapy. Polym Degrad Stab 2019;168:108956.
[187] Cui ZK, Phoeung T, Rousseau PA, Rydzek G, Zhang Q, Bazuin CG, et al. Nonphospholipid fluid liposomes with switchable photocontrolled release. Langmuir 2014;30(36):10818–25.
[188] Chen S, Bian Q, Wang P, Zheng X, Lv L, Dang Z, et al. Photo, pH and redox multi-responsive nanogels for drug delivery and fluorescence cell imaging. Polym Chem 2017;8(39):6150–7.
[189] Razavi B, Abdollahi A, Roghani-Mamaqani H, Salami-Kalajahi M. Light-and temperature-responsive micellar carriers prepared by spiropyran-initiated atom transfer polymerization: investigation of photochromism kinetics, responsivities, and controlled release of doxorubicin. Polymer 2020;187:122046.
[190] Shen H, Zhou M, Zhang Q, Keller A, Shen Y. Zwitterionic light-responsive polymeric micelles for controlled drug delivery. Colloid Polym Sci 2015;293(6):1685–94.
[191] Ramires MCCH, Mattia MB, Tateno RY, Palma LF, Campos L. A combination of phototherapy modalities for extensive lip lesions in a patient with SARS-CoV-2 infection. Photodiagnosis Photodyn Ther 2021;33:102196.
[192] Rywkin S, Ben-Hur E, Malik Z, Prince A, Li YS, Kenney M, et al. New phthalocyanines for photodynamic virus inactivation in red blood cell concentrates. Photochem Photobiol 1994;60(2):165–70.
[193] Zheng Q, He Y, Tang Q, Wang Y, Zhang N, Liu J, et al. An NIR-guided aggregative and self-immolative nanosystem for efficient cancer targeting and combination anticancer therapy. Mol Pharm 2018;15(11):4985–94.
[194] Anugrah DSB, Ramesh K, Kim M, Hyun K, Lim KT. Near-infrared light-responsive alginate hydrogels based on diselenide-containing cross-linkage for on demand degradation and drug release. Carbohydr Polym 2019;223:115070.
[195] Salma SA, Patil MP, Kim DW, Le CMQ, Ahn BH, Kim GD, et al. Near-infrared light-responsive, diselenide containing core-cross-linked micelles prepared by the Diels–Alder click reaction for photocontrollable drug release application. Polym Chem 2018;9(39):4813–23.
[196] Dias LD, Blanco KC, Bagnato VS. COVID-19: beyond the virus. The use of photodynamic therapy for the treatment of infections in the respiratory tract. Photodiagnosis Photodyn Ther 2020;31:101804.
[197] Li M, Sun X, Zhang N, Wang W, Yang Y, Jia H, et al. NIR-activated polydopamine-coated carrier-free "nanobomb" for *in situ* on-demand drug release. Adv Sci 2018;5(7):1800155.

[198] Wu Y, Wang H, Gao F, Xu Z, Dai F, Liu W. An injectable supramolecular polymer nanocomposite hydrogel for prevention of breast cancer recurrence with theranostic and mammoplastic functions. Adv Funct Mater 2018;28(21):1801000.
[199] Deng Y, Käfer F, Chen T, Jin Q, Ji J, Agarwal S. Let there be light: polymeric micelles with upper critical solution temperature as light-triggered heat nanogenerators for combating drug-resistant cancer. Small 2018;14(37):1802420.
[200] Tolstykh GP, Beier HT, Roth CC, Thompson GL, Payne JA, Kuipers MA, et al. Activation of intracellular phosphoinositide signaling after a single 600 nanosecond electric pulse. Bioelectrochemistry 2013;94:23–9.
[201] Kumagai E, Tominaga M, Harada S. Sensitivity to electrical stimulation of human immunodeficiency virus type 1 and MAGIC-5 cells. AMB Express 2011;1(1):1–6.
[202] Kolsek M. TENS-an alternative to antiviral drugs for acute herpes zoster treatment and postherpetic neuralgia prevention. Swiss Med Wkly 2012;142:w13229.
[203] Allawadhi P, Khurana A, Allwadhi S, Navik US, Joshi K, Banothu AK, et al. Potential of electric stimulation for the management of COVID-19. Med Hypotheses 2020;144:110259.
[204] Shi H, Dai Z, Sheng X, Xia D, Shao P, Yang L, et al. Conducting polymer hydrogels as a sustainable platform for advanced energy, biomedical and environmental applications. Sci Total Environ 2021;786:147430.
[205] Qu J, Zhao X, Ma PX, Guo B. Injectable antibacterial conductive hydrogels with dual response to an electric field and pH for localized “smart” drug release. Acta Biomater 2018;72:55–69.
[206] Chen J, Yu M, Guo B, Ma PX, Yin Z. Conductive nanofibrous composite scaffolds based on *in-situ* formed polyaniline nanoparticle and polylactide for bone regeneration. J Colloid Interface Sci 2018;514:517–27.
[207] Uppalapati D, Sharma M, Aqrawe Z, Coutinho F, Rupenthal ID, Boyd BJ, et al. Micelle directed chemical polymerization of polypyrrole particles for the electrically triggered release of dexamethasone base and dexamethasone phosphate. Int J Pharm 2018;543(1–2):38–45.
[208] Woeppel KM, Zheng XS, Schulte ZM, Rosi NL, Cui XT. Nanoparticle doped PEDOT for enhanced electrode coatings and drug delivery. Adv Healthc Mater 2019;8(21):1900622.
[209] Sangsuriyonk K, Paradee N, Sirivat A. Electrically controlled release of anticancer drug 5-fluorouracil from carboxymethyl cellulose hydrogels. Int J Biol Macromol 2020;165:865–73.
[210] Weissig V, Pettinger TK, Murdock N. Nanopharmaceuticals (part 1): products on the market. Int J Nanomedicine 2014:4357–73.
[211] Nyström AM, Fadeel B. Safety assessment of nanomaterials: implications for nanomedicine. J Control Release 2012;161(2):403–8.
[212] Besse HC, Barten-van Rijbroek AD, van der Wurff-Jacobs KM, Bos C, Moonen CT, Deckers R. Tumor drug distribution after local drug delivery by hyperthermia, *in vivo*. Cancers 2019;11(10):1512.
[213] Ma Y, Yu S, Ni S, Zhang B, Kung ACF, Gao J, et al. Targeting strategies for enhancing paclitaxel specificity in chemotherapy. Front Cell Dev Biol 2021;9:626910.
[214] Ulldemolins A, Seras-Franzoso J, Andrade F, Rafael D, Abasolo I, Gener P, et al. Perspectives of nano-carrier drug delivery systems to overcome cancer drug resistance in the clinics. Cancer Drug Resist 2021;4(1):44.